Industrial Chemistry Publication Series
Teknillisen kemian julkaisusarja
Espoo 2007 No. 24

RHODIUM AND COBALT CATALYSTS IN THE HETEROGENEOUS HYDROFORMYLATION OF ETHENE, PROPENE AND 1-HEXENE

Tarja Zeelie (née Kainulainen)

TEKNILLINEN KORKEAKOULU
TEKNISKA HÖGSKOLAN
HELSINKI UNIVERSITY OF TECHNOLOGY
TECHNISCHE UNIVERSITÄT HELSINKI
UNIVERSITE DE TECHNOLOGIE D'HELSINKI

Industrial Chemistry Publication Series
Teknillisen kemian julkaisusarja
Espoo 2007 No. 24

RHODIUM AND COBALT CATALYSTS IN THE HETEROGENEOUS HYDROFORMYLATION OF ETHENE, PROPENE AND 1-HEXENE

Tarja Zeelie (née Kainulainen)

Dissertation for the degree of Doctor of Science in Technology to be presented with due permission of the Department of Chemical Technology for public examination and debate in Auditorium Ke 2 (Komppa Auditorium) at Helsinki University of Technology (Espoo, Finland) on the 16th of November 2007, at 12 o'clock noon.

Helsinki University of Technology
Department of Chemical Technology
Laboratory of Industrial Chemistry

Teknillinen korkeakoulu
Kemian tekniikan osasto
Teknillisen kemian laboratorio

Distribution:

Helsinki University of Technology

Laboratory of Industrial Chemistry

P. O. Box 6100

FI-02015 TKK

Tel. +358-9-4511

Fax. +358-9-451 2622

E-Mail: arja.tuohino@tkk.fi

ISBN 978-951-22-9024-6 (print)
ISBN 978-951-22-9025-3 (pdf, available at http://lib.tkk.fi/Diss/)
ISSN 1235-6840

Edita Prima Oy
Helsinki 2007

ABSTRACT

Hydroformylation is an important commercial process for the conversion of alkenes, carbon monoxide and hydrogen into aldehydes to be further used in the production of various chemicals. The industrial processes operate in a homogeneous mode. Therefore, the development of a solid catalyst would solve problems related to catalyst separation. The purpose of this work was to study supported cobalt and rhodium catalysts in heterogeneous hydroformylation both in liquid and gas-phase conditions. The effect of different preparation methods, precursors, support modifications and pretreatments on the characteristics of the catalysts was investigated.

Atomic layer deposition (ALD) is a promising technique for the preparation of dispersed Co(A)/SiO_2 catalysts using a $Co(acac)_3$ precursor. Higher activity in ethene hydroformylation was obtained with Co(A)/SiO_2 catalysts compared to impregnated Co(N)/SiO_2 catalyst prepared from nitrate precursor. The dispersion, and consequently the activity and oxo-selectivity of the Co(A)/SiO_2 catalyst, was further improved by inert handling of the catalyst. Moreover, by varying the metal content of the Co(A)/SiO_2 catalysts, a clear correlation between metal dispersion and oxo-selectivity was found. The basic AlN modification of the silica support did not enhance hydroformylation activity due to low dispersion of the Co(A)/n·AlN/SiO_2 catalysts.

For the carbon supported catalysts, the best hydroformylation activity was obtained with coconut-shell based Rh/C(C) catalyst. The presence of dispersed active sites and unreduced rhodium enhanced CO insertion, and also unintentional promotion by potassium was possible. Furthermore, without any pretreatment the catalyst exhibited even better propanal yields than with hydrogen pretreatment, apparently due to the better dispersed active sites. Pretreatment with carbon monoxide partially blocked the catalyst surface with carbonaceous residues, which improved CO insertion selectivity, but suppressed the overall activity.

The fibrous polymer-supported Rh-phosphine catalyst, Fibrecat^{TM}, prepared using a $Rh(acac)(CO)_2$ precursor, was the most promising rhodium catalyst in ethene hydroformylation: high propanal selectivity (95%) and high activity were obtained under the mild reaction conditions of 100 ºC and 0.5 MPa. The ^{31}P NMR characterisations suggested the formation of both a Rh-monophosphine species, $Rh(acac)(CO)(PS\text{-}PPh_2)$, and a Rh-bisphosphine species, $Rh(CO)_2(PS\text{-}PPh_2)_2$, on Fibrecat^{TM}, which were transformed in contact with CO/H_2 to the active Rh-carbonyl hydrides.

In the liquid-phase hydroformylation of 1-hexene, the activity of the Rh/C catalysts appeared to correlate with the support: the larger the pores, the better the mass transfer and the higher the activity. In addition, C_{21} products were only formed on a support with sufficiently large pores – an indication of the heterogeneous functionality of the catalysts. With the carbonyl based cobalt catalysts, problems were encountered with the catalyst preparation and handling procedure due to the air sensitivity of the carbonyl precursors.

The Co/SiO_2 catalysts were stable in gas-phase hydroformylation at 173 °C and 0.5 MPa, whereas Rh/C catalysts lost 10-30% of the metal deposited, mostly due to the formation of volatile carbonyls. However, at a lower temperature, i.e. 100 °C and 0.5 MPa, no volatile carbonyls were formed on Fibrecat^{TM}, as confirmed by quantitative ^{31}P NMR characterisations. In liquid-phase conditions, 20–50% of the metal deposited was dissolved from the cobalt and rhodium catalysts. Therefore, the stability of the catalysts in hydroformylation was related to the ability of the catalytic metal to form volatile or soluble carbonyls and thus, to the reaction conditions used.

TIIVISTELMÄ

Hydroformylointi on tärkeä teollinen prosessi, jolla valmistetaan alkeeneista, hiilimonoksidista ja vedystä aldehydejä, joita edelleen käytetään erilaisten kemikaalien tuotannossa. Tällä hetkellä kaupalliset prosessit toimivat homogeenisesti. Kiinteän katalyytin kehittäminen ratkaisisi katalyytin erottamiseen liittyvät ongelmat. Tämän työn tarkoitus oli tutkia kantajalla olevia koboltti- ja rodiumkatalyyttejä sekä neste- että kaasufaasiolosuhteissa. Erilaiset valmistusmenetelmät, prekursorit, kantajan modifiointi, erilaiset katalyytin esikäsittelyt ja näiden vaikutus katalyytin ominaisuuksiin olivat tutkimuksen kohteena.

Atomikerroskasvatustekniikalla (ALD) voidaan valmistaa dispergoituja Co(A)/SiO_2-katalyyttejä käyttäen lähtöaineena $Co(acac)_3$-prekursoria. Näillä katalyyteillä saatiin korkeampi aktiivisuus eteenin hydroformyloinnissa verrattuna impregnoituun Co(N)/SiO_2-katalyyttiin, joka oli valmistettu kobolttinitraatista. Dispersio ja sen seurauksena myös katalyytin aktiivisuus ja oxo-selektiivisyys paranivat, kun katalyyttiä käsiteltiin inertisti. Kun katalyytin metallipitoisuutta kasvatettiin, huomattiin selvä yhteys metallin dispersion ja oxo-selektiivisyyden välillä. Silikan modifiointi emäksisellä AlN-kerroksella ei edistänyt hydroformylointiaktiivisuutta, koska Co(A)/AlN/SiO_2-katalyytin dispersio huononi.

Hiilikantajalle valmistetuista rodiumkatalyyteistä paras aktiivisuus oli kookospähkinäpohjaisella Rh/C(C)-katalyytillä. Dispergoidut aktiiviset kohdat ja pelkistymättömän rodiumin läsnäolo edistivät CO:n insertiota, ja myös tahaton kaliumin promootio oli mahdollinen. Ilman esikäsittelyä saatiin vieläkin parempi propanaalisaanto, koska aktiiviset paikat olivat paremmin dispergoituja. Esikäsittely hiilimonoksidilla osittain tukki katalyytin pinnan hiilijäämillä, mikä paransi CO:n insertioselektiivisyyttä, mutta alensi kokonaisaktiivisuutta.

Polymeerikuidulle valmistettu rodium-fosfiinikatalyytti, Fibrecat™, oli lupaavin katalyytti eteenin hyroformylointiin: korkea propanaaliselektiivisyys (95%) ja korkea aktiivisuus saavutettiin miedoissa reaktio-olosuhteissa 100°C lämpötilassa ja 0.5 MPa paineessa.

^{31}P NMR -karakterisoinneista pääteltiin, että valmistuksen aikana Fibrecat^{TM}-katalyytille muodostuu sekä Rh-monofosfiinia, Rh(acac)(CO)(PS-PPh_2), että Rh-bisfosfiinia, $Rh(CO)_2$(PS-$PPh_2)_2$, jotka CO/H_2-atmosfäärissä muuttuvat aktiivisiksi Rh-karbonyylihydrideiksi.

Rh/C-katalyyttien aktiivisuus 1-hekseenin nestefaasihydroformyloinnissa näytti korreloivan kantajan ominaisuuksien kanssa: mitä isommat huokoset, sitä parempi aineensiirto ja korkeampi aktiivisuus. Myös pitkäketjuisia tuotteita muodostui vain kantajalla, jonka huokoset olivat tarpeeksi isot, mikä oli todiste katalyyttien heterogeenisuudesta. Karbonyylipohjaisilla kobolttikatalyyteillä katalyyttien ilmaherkkyys aiheutti ongelmia katalyyttien valmistuksessa ja käsittelyssä.

Co/SiO_2-katalyytit olivat stabiileja eteenin kaasufaasihydroformyloinnissa (173°C, 0.5 MPa), mutta Rh/C-katalyyteistä hävisi 10-30 % metallista. Alhaisemmassa lämpötilassa (100°C) haihtuvia karbonyylejä ei kuitenkaan muodostunut Rh/kuitu-katalyytillä, mikä todistettiin kvantitatiivisilla ^{31}P NMR -mittauksilla. Nestefaasihydroformyloinnissa koboltti-ja rodiumkatalyyteillä olevasta metallista liukeni 20-50 %. Katalyyttien stabiilisuus hydroformyloinnissa oli siis riippuvainen käytetyn katalyyttimetallin kyvystä muodostaa haihtuva tai liukeneva karbonyyli, ja siten reaktio-olosuhteilla oli vaikutus stabiilisuuteen.

PREFACE

The practical work of this thesis was carried out in the Laboratory of Industrial Chemistry, Helsinki University of Technology, between October 1995 and September 2001, excluding the year 1999. Funding from the Finnish Funding Agency for Technology and Innovation (TEKES), Neste Oil Corporation and Kemira Corporation, through the Synthesis Technology programme, from the Academy of Finland through the Graduate School in Chemical Engineering, from the Nordic Council of Ministers through the Nordic Energy Research Programme and from the Helsinki University of Technology and Fortum Foundation through scholarships is gratefully acknowledged.

I wish to express my warmest thanks to Professor Outi Krause for the opportunity to work with this challenging topic, and for her guidance during these years. I am most grateful to my co-author and supervisor Dr. Marita Niemelä for her enthusiasm and advice during my research and for getting me started with my postgraduate studies. I am greatly indebted to my coauthors Dr. Riikka Puurunen for preparing the Co/AlN/SiO_2 catalysts and to Dr. Andrew Root for measuring the NMR spectra. Special thanks to Mr. Leif Backman for the chemisorption measurements, Mr. Hannu Revitzer for rhodium analyses, Mrs. Mari Halttunen for preparing the Rh/C catalysts and Dr. Mary Metzler for revising the language of the thesis. Former Smoptech Ltd. is thanked for providing the fibre supported catalysts.

I thank my colleagues and the personnel of the Laboratory of Industrial Chemistry for creating a pleasant and motivating working atmosphere. Thank you for all the invaluable help I have received. And finally, warmest thanks go to my family and friends for their support during these years, to Ernest for his encouragement and support, and to Christian, Hester and Konsta for the joy they have brought into my life.

Espoo, May 2007

Tarja Zeelie

LIST OF PUBLICATIONS

This thesis is based on the following appended publications, which are referred to in the text by their Roman numerals:

I Kainulainen, T. A., Niemelä, M. K. and Krause, A. O. I., Ethene hydroformylation on Co/SiO_2 catalysts, *Catal. Lett.* **53** (1998) 97-101.

II Puurunen, R. L., Zeelie, T. A. and Krause, A. O. I., Cobalt(III) acetylacetonate chemisorbed on aluminum-nitride-modified silica: characteristics and hydroformylation activity, *Catal. Lett.* **83** (2002) 27-32.

III Kainulainen, T. A., Niemelä, M. K. and Krause, A. O. I., Rh/C catalysts in ethene hydroformylation: the effect of different supports and pretreatments, *J. Mol. Catal. A: Chem.* **140** (1999) 173-184.

IV Zeelie, T. A., Root, A., Krause, A. O. I., Rh/fibre catalyst for ethene hydroformylation: Catalytic activity and characterisation, *Appl. Catal. A: Gen.* **285** (2005) 96-109.

V Kainulainen, T. A., Niemelä, M. K. and Krause, A. O. I., Hydroformylation of 1-hexene on Rh/C and Co/SiO_2 catalysts, *J. Mol. Catal. A: Chem.* **122** (1997) 39-49.

Contribution of Tarja Zeelie (née Kainulainen) to publications I-V:

I, III She defined the research plan and carried out the experiments. She analysed the results, and was a major contributor in interpreting the results as well as writing of the manuscript.

II She carried out the hydroformylation experiments, wrote the first version of the manuscript together with R. L. Puurunen and contributed to the final version of the manuscript.

IV She defined the research plan, carried out the hydroformylation experiments, measured the DRIFT spectra, interpreted the results (except for the NMR spectra), wrote the first version of the manuscript and after discussion with the co-authors, wrote the final version of the manuscript.

V She defined the research plan together with the co-authors and carried out the experiments. She was the main author and a major contributor in both interpreting the results and writing of the manuscript.

ABBREVIATIONS AND SYMBOLS

AAS	Atomic absorption spectroscopy
acac	Acetylacetonate (pentane-2,4-dionate), $C_5H_7O_2^-$
(Acet)	Acetone
ALD	Atomic layer deposition
AlN	Aluminium nitride
a.u.	Arbitrary units
C_{14}	Hemiacetals, aldols and aldehydes containing 14 carbon atoms
C_{21}	Acetals, aldols and aldehydes containing 21 carbon atoms
C(C)	Coconut based active carbon from Johnson Matthey
C(N)	Peat based active carbon Norit Rox 0.8
C(T)	Wood based active carbon from Takeda Shirasaki
C_6-O	Condensation products of propanal (containing 6 carbon atoms)
Co(A)	Cobalt acetylacetonate, $Co(acac)_3$
2Co(CO)	Dicobalt octacarbonyl, $Co_2(CO)_8$
4Co(CO)	Tetracobalt dodecacarbonyl, $Co_4(CO)_{12}$
CPMAS	Cross-polarisation magic angle spinning
dcm	Dichloromethane
DRIFT	Diffuse reflectance Fourier transform infrared (spectroscopy)
DOP	Dioctyl phtalate
FID	Flame ionisation detector
Hacac	Acetylacetone (pentane-2,4-dione), $C_5H_8O_2$
ICP	Inductively coupled plasma
INAA	Instrumental neutron activation analysis
LPO process	Low pressure oxo process
mono/bis ratio	Molar ratio of the Rh-monophosphine species to the Rh-bisphosphine species
MS	Mass spectrometer
n.d.	not determined
n/i ratio	normal to branched ratio of product aldehydes
NMR	Nuclear magnetic resonance (spectroscopy)

(N)	Nitrate
(p)	Pentane
PS	Polystyrene
PVC	Polyvinyl chloride
Rh/C(COMM)	Commercial active carbon supported rhodium catalyst
S	Selectivity, mol-%
SEM	Scanning electron microscopy
S_{oxo}	Sum of selectivities for propanal, propanol and C_6-O
TCD	Thermal conductivity detector
TEM	Transmission electron microscopy
THF	Tetrahydrofuran
TMA	Trimethylaluminium, $Al(CH_3)_3$
TPD	Temperature programmed desorption
TPPTS	Triphenylphosphine trisulphonate
TPR	Temperature programmed reduction
WHSV	Weight hourly space velocity, h^{-1}
X	Conversion, %
XPS	X-ray photoelectron spectroscopy
XRD	X-ray diffraction
Y	Yield, mol-%

RHODIUM AND COBALT CATALYSTS IN THE HETEROGENEOUS HYDROFORMYLATION OF ETHENE, PROPENE AND 1-HEXENE

1 INTRODUCTION

1.1 Industrial hydroformylation

The hydroformylation reaction (OXO process) converts alkenes, carbon monoxide and hydrogen into aldehydes by increasing the chain-length of the reacting alkene by one carbon (Scheme 1). Both linear and branched aldehydes are formed, which are further converted to alcohols, carboxylic acids, acroleins, diols, amines, acetals and aldol condensation products. Hydroformylation products are raw materials for a variety of bulk and speciality chemicals, mainly for plasticizers and detergents, and thus, hydroformylation has special significance for the polymer industry. Hydroformylation could be utilised in organic synthesis as well since various functional alkenes can be used as reactants [1].

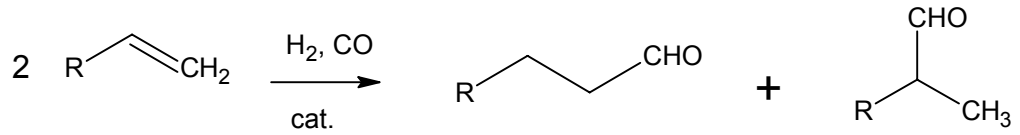

Linear or normal product (n)

Branched or iso product (i)

Scheme 1. Hydroformylation reaction.

In principle, all the transition metals capable of forming carbonyls are potential catalysts for homogeneous hydroformylation. The hydroformylation activity of unmodified metals decreases in the order: Rh >> Co > Ir, Ru > Os > Pt > Pd > Fe > Ni [2]. Only rhodium and cobalt are used commercially and rhodium is 10^3 - 10^4 times more active than cobalt.

The hydroformylation reaction was discovered in 1938 by Otto Roelen, and from the mid-1950s the importance of the reaction has steadily increased [3]. The first generation of hydroformylation catalysts was based on cobalt carbonyl. Since the reactivity of cobalt is low, harsh reaction conditions had to be used. The second generation processes use

rhodium as the metal. The first ligand-modified rhodium process came into use commercially in 1974 (Celanese) and was soon followed by others, in 1976 by Union Carbide Corporation (UCC) and in 1978 by Mitsubishi Chemical Corporation. They all used triphenyl phosphine (PPh_3) as the ligand. The UCC process is often referred to as the low pressure oxo (LPO) process. The advantages of the LPO process were mild reaction conditions, simpler and therefore cheaper equipment, high efficiency and high yield of normal products [4]. Also, the pronounced thermal stability of rhodium-phosphine complexes made the recovery of the catalyst easier [4]. Thus, since the mid-seventies the rhodium catalysts started to replace the cobalt catalysts in propene and butene hydroformylation. Approximately 66% of the world-wide capacity in hydroformylation processes in 1997 (7.6 million tons) was based on the LPO process that yields n-butanal [5]. 70% of n-Butanal is in turn converted to dioctyl phthalate (DOP), which is used as a plasticiser in the production of PVC. The LPO process has been improved by the use of bisphosphite-modified rhodium catalysts with higher activity and selectivity for the normal product [6]. The first commercial plant was started in 1995 by UCC.

For hydroformylation of higher olefins, however, cobalt dominates rhodium by a 9:1 ratio (1995) mainly for two reasons. The first reason is the low reactivity of rhodium with branched olefins containing partially internal carbon double bonds. The second reason is the high boiling points of the product aldehydes that prevent product separation by distillation, as too much thermal strain is imposed on the rhodium catalyst. Thus, C_7–C_{11} branched alcohols used for plasticizer production and linear C_{12}–C_{16} alcohols used as detergent alcohols are mostly produced using cobalt-based processes [3].

The third-generation process offered an elegant solution to the catalyst separation using a two-phase system. The Ruhrchemie/Rhone-Poulenc process established in 1984 on an industrial scale for the hydroformylation of propene by Celanese and in 1995 for the hydroformylation of 1-butene uses a water-soluble Rh-TPPTS (triphenylphosphine trisulphonate) catalyst [3, 4]. The water-soluble catalyst in the aqueous phase is easily separated from the product aldehydes that are in the organic phase. The fourth generation process for large-scale applications still has to be selected from the potential candidates. It will concern higher alkenes only since propene hydroformylation processes are already

highly developed. In recent years, platinum and palladium have been studied for the hydroformylation of higher alkenes, the latter showing promising results [3]. Phosphite-based catalysts and new diphosphines have also been reported for the conversion of internal alkenes to terminal products [3]. Lately, interest in the production of fine chemicals such as expensive vitamins, medicines, perfumes, herbicides and nutrition additives by hydroformylation of very different substrates has increased [1].

1.2 Heterogenisation of catalysts

Homogeneous catalysts are highly active and selective, but they have several disadvantages: problems with separation of the catalyst from reaction products, expensive metal losses, solubility limitations and corrosivity of catalytic solutions. For rhodium catalysis, economical operation requires recovery at ppb level due to the high cost of rhodium. Therefore, several attempts have been made to heterogenise homogeneous catalysts on a solid support.

The heterogenised catalysts can be divided into two groups: immobilised metal complex catalysts and supported metal catalysts [7]. The immobilised metal complex catalysts can be further divided into supported and anchored metal complex catalysts, as summarised in Table 1. The coordinatively anchored metal complex catalysts, where metal complexes are chemically bonded to the functional groups of the support, are the most promising option for immobilised catalysts (Figure 1). The strong bonding of the complex to the support through the functional groups, and the possibility for modification of the support properties at the same time, are the obvious advantages compared to other types of immobilised metal complex catalysts. The most commonly used functional groups are phosphine ligands that are bonded via a methylene chain to an oxide surface or an organic macromolecule. Table 2 shows some examples of coordinatively anchored metal complex catalysts employed in the hydroformylation of alkenes.

Table 1. Classification of immobilised metal complex catalysts [7].

1. Supported metal complex catalysts
• Catalysts containing a dispersed phase of complex on a support *Physical adsorption* • Supported Liquid-Phase Catalysts (SLPC) • Supported Aqueous-Phase Catalysts (SAPC) *Capillary condensation*
2. Anchored metal complex catalysts *Chemical bonding*
• Ion exchange • Covalent grafting Metal complex bonded to oxygen atoms on an oxide support surface • Coordinative anchoring Metal complex anchored on a chemically modified support containing functional groups of donor-acceptor type

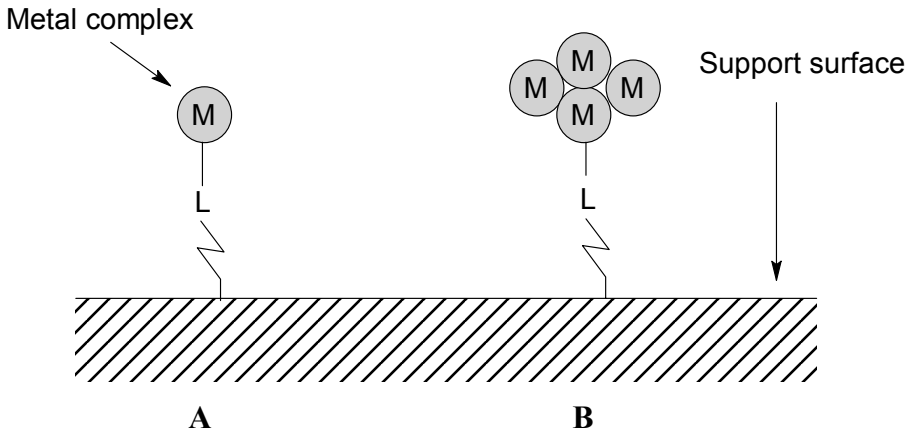

Figure 1. Coordinative anchoring of a metal complex to the support surface, A is a mononuclear complex, B is a polynuclear complex, L is a ligand.

Table 2. Examples of coordinatively anchored metal complexes for hydroformylation of alkenes.

Support; linking agent[a]	**Precursor**	**Reactant (Reaction conditions)**	**Ref.**
3-aminopropyltriethoxysalane-co-tetraethoxysalane; PPh_2	$[Rh(CO)_2Cl]_2$	1-hexene (90–120 °C, 3–6 MPa)	[8]
Functionalised zeolite Na-Y, Si–MCM-41 and Si–MCM-48	$HRh(CO)(PPh_3)_3$	1-octene, styrene (100 °C, 4 MPa)	[9]
cellulose acetate and poly(phenyl)sulphone films; PPh_3	$HRh(CO)(PPh_3)_3$	ethene, propene (80 °C, 0.1 MPa)	[10]
2-20% cross-linked PS/DVB	$RhCl(CO)(PPh_3)_2$	propene (100 °C , 1.43 MPa)	[11]
PS-PPh_2/SiO_2	$RhCl(CO)_2$	ethene, propene, 1-butene (130 °C, 0.1 MPa)	[12]
polymeric organosiloxanes styrene-co-4-N-pyrrolidinopyridine	$Rh(acac)(CO)_2$ $RhCl_3 \cdot 3H_2O$	isobutene, 1-hexene (120 °C, 6 MPa)	[13]
1%DVB	$Ru(CO)_3(PPh_3)_2$	1-pentene (140 °C, 7 MPa)	[14]
2% cross-linked DVB/PS; PPh_2	$[RhCl(COD)]_2$	1-heptene (70 °C, 3 MPa)	[15]
poly(vinyl benzyl diethylenetriamine)	$[Rh(CO)_2Cl]_2$	1-hexene (30–110 °C, 2–8 MPa)	[16]
PS/1-2%DVB; PPh_2	$RhH(CO)(PPh_3)_3$	allyl alcohol (40–120 °C, 0.3–5.5 MPa)	[17]
poly(styrene-co-p-t-butoxy-carbonyl-oxystyrene), poly(styrene-co-p-hydroxystyrene); phosphite groups	Rh(COD)(acac)	cyclo-octene (80 °C, 2 MPa)	[18]
poly(arylene ether triphenyl phosphine)	$Rh(acac)(CO)_2$	1-octene (120 °C, 1.7 MPa)	[19]
poly(propylene-g-p-styryldiphenylphosphine)	$Rh(acac)(CO)_2$	1-hexene (45–85 °C, 1 MPa)	[20]
styrene/DVB; PPh_2	$Co_2(CO)_6$	Pentene (144–172 °C, 2.8–6.9 MPa)	[21]

[a]PS = polystyrene; DVB = divinylbenzene; COD = cyclo-octadiene

The supported metal catalysts are prepared by impregnating metal salts and oxides on the support followed by reduction, or by decomposition of organometallic compounds on the support. For instance, active carbon, silica, alumina or zeolites can be used as supports onto which e.g. the metal nitrates are impregnated. Both rhodium and cobalt, separately and together, in combination with other metals on various supports have been studied in the hydroformylation of ethene [22, 23] and higher alkenes [24– 27].

Even though the heterogenisation of the homogeneous precursors often results in a decrease in activity, it has also resulted in improved performance. Polymers modified with phosphines or phosphites have been studied for hydroformylation of various reactants both with rhodium and cobalt catalysts as illustrated in Table 2. Greater normal/branched ratios (n/i) of the product aldehydes have been obtained on polymer-supported phosphine-modified catalysts compared to homogeneous catalysts, possibly due to a higher localised concentration of phosphine atoms around the rhodium centre compared to the free solution [10, 20, 28].

In liquid-phase applications, leaching of the active metal into the liquid phase [16, 29, 30] has prevented the commercial use of heterogenised catalysts. In gas-phase hydroformylation, the use of supported metal catalysts is more feasible, since the operating conditions are mild: the reaction can be carried out at low pressures (and below 150 ºC) where the competing Fischer-Tropsch reaction ceases. Moreover, hydroformylation can be used as a test reaction for Fischer-Tropsch catalysts to determine their ability to form oxygenates.

1.3 Reaction mechanism

In the early 1960s Heck and Breslow [5] formulated the generally accepted hydroformylation cycle for cobalt catalysis that is also valid for unmodified rhodium catalysts. The hydroformylation mechanism for phosphine-modified rhodium catalysts follows, with minor modifications, the Heck-Breslow cycle. According to Wilkinson [2], two possible pathways are imaginable: the associative and the dissociative mechanisms. It

is accepted today that Wilkinson's dissociative mechanism is the likely kinetic path for hydroformylation [1, 2]. This is shown in Scheme 2. The active species are 16-electron hydrides of the general formula $HRh(CO)_x(PPh_3)_{3-x}$ (x = 1, 2) formed by the dissociation of CO from the 18-electron carbonyl hydride [2, 31]. The basic steps in the hydroformylation reaction after the initial formation of the hydrido metal carbonyl are: (1) dissociation of CO to form the unsaturated 16-electron species, (2) coordination of alkene, (3) formation of the alkylmetal carbonyl species, (4) coordination of CO, (5) insertion of CO to form the acylmetal carbonyl, (6) oxidative addition of hydrogen, and (7) cleavage of the acylmetal species by hydrogen to form the aldehyde and regeneration of the hydridometal carbonyl. It is generally believed that the oxidative addition of hydrogen to the rhodium-acyl complex (step 6 in Scheme 2) is the rate determining step [2]. Leeuwen [3] has proposed that, roughly speaking, in phosphine catalyst systems the migratory insertion of the alkene into Rh-H (step 3 in Scheme 2) is the rate-determining step under standard industrial process conditions.

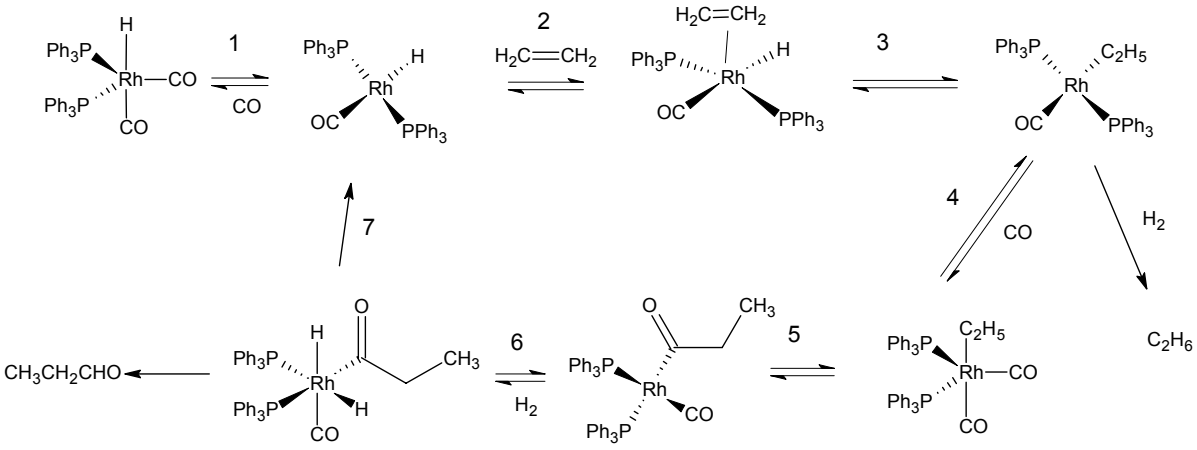

Scheme 2. Wilkinson's dissociative mechanism presented for rhodium-phosphine catalysed ethene hydroformylation [2, 31].

The reaction mechanism on supported catalysts follows a similar mechanism. Henrici-Olivé and Olivé [32] have suggested that the decisive difference between the homogeneous and the heterogeneous process is the availability of a free, mobile, very reactive hydrido-metal species in solution. According to them, the last step (steps 6 and 7 in Scheme 2), the transformation of the acyl-metal species to the aldehyde, proceeds through reaction with a

second catalyst species in homogeneous media, but in heterogeneous media the oxidative addition of molecular hydrogen to an acyl-metal species is the only means of formation of the aldehyde. The hydrogenation of the acyl intermediate was identified as the rate determining step at 0.1 MPa on Rh/SiO_2 [33].

In some studies, the CO insertion selectivity on supported unmodified metal catalysts, is related exclusively to the linearly adsorbed CO on isolated Rh^0 sites [34], whereas other studies show that reaction rate and selectivity for hydroformylation increases in the presence of Rh^+ sites [35]. Thus, the dispersion of the catalytic metal and the extent of reduction are the main factors determining the CO insertion activity, and thereby, the selectivity towards aldehyde formation. According to Sachtler and Ichikawa [36], two types of active sites are responsible for aldehyde formation: isolated, partially oxidised metal crystallites for the migratory CO insertion into metal alkyl bonds, and fairly large metal ensembles for the dissociation of hydrogen. Hedrick et al. [37, 38] noticed that on a Mn-Rh/SiO_2 catalyst, spill-over hydrogen from the metal to the silica surface plays a role in the hydrogenation of the acyl intermediate. Thus, the hydrogenation of ethyl species to form ethane, and the hydrogenation of adsorbed acyl species to form propanal, are involved with two different types hydrogen: metal adsorbed hydrogen and hydrogen from Si-OH, respectively.

1.4 Scope of the research

The goal of this research was to develop a solid catalyst for heterogeneous hydroformylation. Rhodium and cobalt are the most active transition metals for hydroformylation and they were obvious choices for the catalytic metals for the preparation of the solid catalysts. Silica was chosen, because it is an inert, cheap support material widely applied in catalysis. Active carbons have many features that make them good candidates as supports, including high surface area, which together with the pore structure, can be varied relatively easily. Also, carbon is inexpensive, inert in corrosive environments, and precious metals supported on it can be easily recovered.

Both in Fischer-Tropsch synthesis and in ethene hydroformylation, CO insertion necessary for the formation of oxo-products is associated with isolated catalytic metal sites. Atomic layer deposition (ALD) was chosen as one of the preparation techniques for the preparation of Co(A)/SiO_2 catalysts since highly dispersed catalysts have been obtained with this method [39]. For comparison, impregnated Co/SiO_2 and Rh/SiO_2 catalysts were prepared and tested. Moreover, a completely new catalyst support, AlN/SiO_2, prepared by the ALD technique, was used for the preparation of Co(A)/AlN/SiO_2 catalysts in order to test the effect of a basic additive on hydroformylation activity.

In homogeneous processes, phosphines are used to direct the selectivity of the products towards aldehydes and to increase the amount of the straight-chain aldehyde compared to the branched one. In a similar way, we wanted to improve the oxo-selectivity of our catalysts by modifying the support with phosphines. A polymeric phosphine-containing fibre support was prepared by a pre-irradiation grafting method. A Rh(acac)$(CO)_2$ precursor was coordinatively anchored on the phosphine groups of the fibre support. A silica-supported Rh-phosphine catalyst was prepared and tested for comparison.

In addition to the industrial importance of ethene hydroformylation, it offers the possibility of studying CO insertion in gas-phase conditions. The results can subsequently be applied to higher alkenes hydroformylation. Moreover, ethene hydroformylation offers a way to test oxygenate formation capability of the Fischer-Tropsch synthesis catalysts. Ethene hydroformylation is a simple test reaction for the study of the interactions between dispersion, the extent of reduction and CO insertion activity.

Preliminary propene hydroformylation experiments were carried out in order to assess the formation of normal to branched aldehydes with rhodium catalysts. The activity of the cobalt and rhodium catalysts in liquid-phase conditions was studied in 1-hexene hydroformylation. The determination of the stability of the catalysts both in gas and liquid-phase conditions was an important part of this work.

2 EXPERIMENTAL

2.1 Preparation of catalysts

Two different preparation methods were used in the preparation of the cobalt and rhodium catalysts: impregnation and atomic layer deposition (ALD). The supports used for the preparation of the catalysts were silica, activated carbon, AlN/SiO_2 supports prepared by ALD and polymeric phosphine-containing fibre support prepared by a pre-irradiation grafting method. Table 3 presents the catalysts prepared for hydroformylation, precursors, supports and preparation methods used as well as conditions for activation of the catalysts before the hydroformylation reaction. For all the catalysts, the metal content is used as a prefix in the name of the catalyst.

ALD is a technique to prepare catalysts by saturative chemisorption and is described in more detail by Puurunen [40]. The general steps in the preparation of materials are as follows:

Initiation: Stabilisation of the reactive sites on the surface typically carried out by a heat treatment.

- ✓ Physisorbed molecules, most often water adsorbed from ambient air are removed.

Step 1: Saturating reaction of a gaseous reactant (typically a metal compound) with the reactive sites of the support surface.

- ✓ The reaction is allowed to proceed until the surface is saturated with the adsorbing species and no more reaction takes place. Thereafter, excess reactant and possible gaseous reaction products are removed by an inert gas purge or by evacuation.

Step 2: Saturating reaction of another reactant (typically a non-metal compound) with the reactive sites of the support.

- ✓ The adsorbed species left behind by the first reactant form a major part of the reactive sites. Excess reactant and the gaseous reaction products are removed.

Steps 1 and 2 are referred to as a reaction cycle and are repeated to increase the amount of adsorbed species.

Table 3. Catalysts studied in hydroformylation.

Catalyst	**Precursor**	**Support**	**Solvent/ Method**	**Activation**	**Ref.**
$Co(N)/SiO_2$	$Co(NO_3)_2{\cdot}6H_2O$	Grace 432	water/ Impr.	H_2, 400 ºC, 1 h/ 7 h	I, V
$2Co(CO)(p)/SiO_2$	$Co_2(CO)_8$	Grace 432	pentane/ Impr.	H_2, 300 ºC, 7 h	V
$2Co(CO)(dcm)/SiO_2$	$Co_2(CO)_8$	Grace 432	DCM/ Impr.	H_2, 300 ºC, 7 h	V
$4Co(CO)(dcm)/SiO_2$	$Co_4(CO)_{12}$	Grace 432	DCM/ Impr.	H_2, 300 ºC, 7 h	V
$Co(A)/SiO_2$	$Co(acac)_3$	Grace 432	- /ALD	H_2, 550 ºC, 7 h	I, II
$Co/n{\cdot}AlN/SiO_2$	NH_3, TMA $Co(acac)_3$	Grace 432	- /ALD	H_2, 550 ºC, 7 h	II
Rh/SiO_2	$Rh(NO_3)_3{\cdot}2H_2O$	Grace 432	water/ Impr.	H_2, 300 ºC, 3 h	IV
Rh/C(N)	$Rh(NO_3)_3{\cdot}2H_2O$	Norit Rox 0.8	water/ Impr.	H_2, 400 ºC, 1 h/ CO 400 ºC, 1 h	III, V
Rh/C(T)	$Rh(NO_3)_3{\cdot}2H_2O$	Takeda Shirasaki	water/ Impr.	H_2, 400 ºC, 1 h/ CO 175 ºC, 1 h	III-V
Rh/C(C)	$Rh(NO_3)_3{\cdot}2H_2O$	Johnson Matthey	water/ Impr.	H_2, 400 ºC, 1 h/ CO 400 ºC, 1 h	III-V
$Rh\text{-}PPh_3/SiO_2$	$Rh(acac)(CO)(PPh_3)$	Grace 432	DCM/ Impr.	-	IV
Fibrecat™	$Rh(acac)(CO)_2$	polymeric fibre[a]	DCM or acetone/ Impr.	Ar, 100 ºC/110 ºC, 1–7 h H_2, 100 ºC/110 ºC, 7 h CO, 100 ºC/110 ºC, 3–7 h H_2/CO, 100 ºC/110 ºC,7 h	IV

[a]polyethene(g-styrene-co-styryldiphenyl-phosphine)

2.1.1 Cobalt catalysts

The supports used for the preparation of the cobalt catalysts were silica and silica modified with AlN. For the Co/SiO_2 catalysts, porous Grace Davidson 432 silica with a particle size of 0.5–1.0 mm, surface area of 320 m^2/g and a pore volume of 1.2 cm^3/g was used as the support. The silica support was pretreated with a volumetric 1:1 mixture of ethanol and water in order to equalize the OH^- group distribution of the carrier before impregnation. The $Co(N)/SiO_2$ catalyst [I] was prepared by impregnation from an aqueous solution of $Co(NO_3)_2 \cdot 6H_2O$ and calcined under air flow at 300 °C for 12 h.

The carbonyl based Co/SiO_2 catalysts were prepared by incipient wetness impregnation using dichloromethane or pentane as solvent and $Co_2(CO)_8$ and $Co_4(CO)_{12}$ as precursors [V]. The silica support was dehydroxylated at 600 °C under vacuum. All stages of the preparation of the carbonyl catalysts were carried out under an inert atmosphere.

Cobalt(III)acetylacetonate, $Co(acac)_3$ (acac = acetylacetonate, pentane-2,4-dionato) was used as the precursor in the ALD preparation [41]. Catalyst preparation consisted of the following steps: (i) preheating of the silica support in air for 16 h at 600 °C, (ii) chemisorption of the gaseous precursor up to surface saturation, and (iii) removal of the remaining ligands by calcination in synthetic air (450 ºC, 4 h) for all but the last deposition. The steps (ii) and (iii) were repeated in order to obtain higher cobalt content. The catalysts after one (5 wt%), three (11 wt%) or five (16 wt%) preparation cycles are denoted as 5-$Co(A)/SiO_2$, 11-$Co(A)/SiO_2$ or 16-$Co(A)/SiO_2$, respectively [I].

The AlN/SiO_2 supports were prepared in an ALD reactor. Details of the preparation are given in paper [II], but here they are only presented in brief. Porous Grace Davidson 432 silica (288 m^2/g) with a particle size of 315–500 μm was used as the support. The AlN/SiO_2 samples were prepared in the reactor in three steps: (i) precalcination of the silica in ambient air at 750 ºC for 16 h and subsequently in the reaction chamber at 550 ºC for 3 h, (ii) reaction of TMA with the support at 150 ºC, and (iii) reaction of ammonia with the TMA-modified sample, starting at 150 ºC and terminating at 550 ºC. Steps (ii) and (iii) were repeated up to six times to increase the concentration of AlN. In the sample code,

"*n*·AlN/SiO_2" the *n* denotes how many times the step was repeated. Silica preheated at 750 ºC and the 2·AlN/SiO_2 and 6·AlN/SiO_2 samples were used as supports for the cobalt catalysts. $Co(acac)_3$ was vaporised at 170 ºC and allowed to react with the supports at 180 ºC. The catalyst preparation and handling was carried out with an inert atmosphere, as was preparation of the 5-Co(A)/SiO_2(inert) prepared as a reference catalyst.

2.1.2 Rhodium catalysts

The supports used for the preparation of the rhodium catalysts were silica, active carbon, and polymeric phosphine-containing fibre prepared by the pre-irradiation grafting method. For the preparation of the silica supported rhodium catalysts, the same Grace Davidson 432 silica was used as a support as was used for the Co/SiO_2 catalysts. For the preparation of the 6-Rh/SiO_2 catalyst, the silica support was pretreated with a volumetric 1:1 mixture of ethanol and water and dried overnight at 120 °C and further in vacuum at 0.1–0.4 kPa and 210 °C for 4 h. The 6-Rh/SiO_2 catalyst [IV] was prepared by impregnation from an aqueous solution of $Rh(NO_3)_3 \cdot 2H_2O$ and calcined under 5% O_2/N_2 flow at 400 ºC for 6 h.

For the preparation of 2-Rh-PPh_3/SiO_2 [IV] (Smoptech Ltd), the silica support was dried for 1 h at 250 °C and allowed to cool to room temperature under vacuum before the incipient wetness impregnation. The Rh(acac)(CO)PPh_3 precursor was dissolved in dichloromethane under nitrogen and added to the support with mixing. The catalyst was dried under vacuum to constant weight.

The Rh/C catalysts [III-V] were prepared by impregnation from an aqueous solution of $Rh(NO_3)_3 \cdot 2H_2O$ [42]. Peat based Norit Rox 0.8 (N), coconut based carbon from Johnson Matthey (C) and wood based Takeda Shirasaki (T) were used as active carbon supports. The Rh/C catalysts were calcinated under flowing nitrogen for 3 h at 400 °C. The rhodium contents of the catalysts were 3–7 wt%.

The Rh/fibre catalysts (Fibrecat^{TM}) [IV] were supplied by former Smoptech Ltd. The crosslinked polyethene fibre was grafted with styrene and *p*-styryldiphenylphosphine by the

pre-irradiation grafting method using high energy electrons [43]. A $Rh(acac)(CO)_2$ precursor was coordinatively anchored from dichloromethane or acetone solution onto the fibre support. The metal loading of Fibrecat™ varied from 3 to 7.7 wt% rhodium. The phosphorus content of the catalysts was between 0.4 and 1.0 mmol $P/g_{catalyst}$. The length of the fibre was < 0.25 mm and the diameter was 20 μm.

2.2 Characterisation of catalysts

The characterisations of the catalysts are presented in detail in publications I-V. The metal content of the catalysts before and after the reaction was determined by atomic absorption spectroscopy (AAS) [I-V], instrumental neutron activation analysis (INAA) [III] or inductively coupled plasma (ICP) [IV]. The carbon loading of the samples was measured with a LECO analyser by burning at 950 °C in air [I, II] or with a Ströhlein analyser by burning at 1350 °C with oxygen [II]. The nitrogen loading of the samples was measured with a LECO analyser [II]. The metal particle sizes were estimated from H_2 [I-IV] and CO chemisorption measurements [III, IV], and the extent of reduction was determined by X-ray photoelectron spectroscopy (XPS) [III, V] or oxygen titration [I, IV]. The reducibility of the Rh/C catalysts was studied by temperature programmed reduction (TPR) with hydrogen [III]. Fibrecat™ was characterised by ^{31}P nuclear magnetic resonance (NMR), ^{13}C NMR and diffuse reflectance Fourier transform infrared (DRIFT) spectroscopies [IV].

2.3 Reaction tests

2.3.1 Vapour-phase hydroformylation of ethene and propene

The ethene hydroformylation studies were carried out in an automated fixed bed tubular reactor in vapour phase at 0.5–1.0 MPa and 75–175 °C as described in detail in papers [I-IV]. The total feed of 3.5 or 7 dm^3/h consisted of argon, carbon monoxide, hydrogen and ethene in molar ratio 1:2:2:2. Weight hourly space velocity (WHSV) for ethene feed at

standard reaction conditions (25 °C, 0.1 MPa) was 2.5–5 h^{-1}. The catalyst, in the amount of 0.5 or 1 g, was in some cases diluted with glass beads in a 1:1 volume ratio, and in situ pretreatments were carried out as described in Table 3. The reactor was a stainless steel tubular reactor. The temperature measurement was carried out by three calibrated K-type thermocouples inside the thermocouple pocket and with one movable thermocouple for the measurement of the axial temperature profile of the reactor. The thermocouple pocket was inside the catalyst bed.

Product analysis was carried out on-line by two HP 5890 series gas chromatographs. The argon, carbon monoxide and ethene were analysed by a thermal conductivity detector (TCD) using packed column filled with activated carbon coated with 2% squalane. The separation of the products was carried out by a DB-1 column (J&W Scientific) and a PoraplotQ column (Hewlett Packard) and two flame ionisation detectors (FIDs). The surface areas of the peaks were divided by sensitivity factors as given by Dietz [44] and normalised to obtain the distribution of the products in weight percentages.

The reaction time was usually 24 hours, but sometimes longer times (max. 70 hours) were used to observe the long-term performance of the catalysts. Conversion (X), selectivity (S) and yield (Y) were based on the molar amount of ethene consumed. The main reaction products in vapour-phase hydroformylation of ethene [I-IV] were ethane, propanal, n-propanol and secondary C_6 oxygenates (C_6-O): 2-methyl-2-pentenal, 2-methyl-1-pentanal and 2-methyl-1-pentanol, formed by aldol condensation and subsequent dehydration and hydrogenation. With cobalt catalysts, small amounts of C_3-C_{11} hydrocarbons, propanoic acid and methane were also formed [I, II]. In addition, with Rh/C catalysts, small amounts of 3-pentanone, propylformate and propylpropionate were detected [III]. The condensation products of propanal are denoted by C_6-O, and the oxo-selectivity (S_{oxo}) is defined as the sum of selectivities for propanal, propanol and C_6-O.

The same reactor and analysis system as used for ethene hydroformylation was used for propene hydroformylation experiments. The reaction was carried out in vapour phase at 0.3–0.6 MPa and 90–150 °C. The total feed of 7.0 dm^3/h consisted of argon, carbon

monoxide, hydrogen and propene in a molar ratio of 4:1:1:1. WHSV for propene feed at standard reaction conditions (25 °C, 0.1 MPa) was 3.4 h^{-1}. The catalyst amount used was 0.5 g. In situ pretreatments were carried out as described in Table 3. Conversion, selectivity and yield were based on the molar amount of propene consumed. The main reaction products in the vapour-phase hydroformylation of propene were propane, n-butanal and i-butanal. The analysis of the products was carried out in the same way as for ethene hydroformylation described above.

2.3.2 Liquid-phase hydroformylation of 1-hexene

The liquid-phase experiments [V] were carried out in a high-pressure autoclave at an initial pressure of 7.3 MPa ($CO:H_2$ = 1:1) and temperature of 150 °C for 3–4 h. The reaction vessel was a 250 cm^3 AISI316 magnetically stirred autoclave, equipped with a separate zirconium or teflon vessel. The reduced catalyst and 1-hexene were packed into the reaction vessel in a glove box under a nitrogen atmosphere, and then transferred to the autoclave. At the end of the experiment, the autoclave was cooled to room temperature and depressurised.

The products were diluted with tetrahydrofuran (THF) and analysed by an HP 5890 series gas chromatograph, using a polar DB WAX capillary column and FID. The surface areas of the peaks were divided by sensitivity factors as given by Dietz [44] and normalised to obtain the distribution of the products in weight percentages.

The isomerisation products of 1-hexene could not be detected with the analysis procedure used. Thus, in the calculations, conversion, selectivity and yield were based on the total amount of hexenes consumed. The main reaction products were hexane, n-heptanal, 2-methyl-hexanal, 2-ethyl-pentanal, and the corresponding alcohols, n-heptanol, 2-methyl-hexanol and 2-ethyl-pentanol. The secondary products are denoted by C_{14} or C_{21} including mainly condensation or acetalisation products, respectively.

3 HYDROFORMYLATION OF ETHENE

3.1 Cobalt catalysts

3.1.1 Characteristics of cobalt catalysts

Dispersion and the extent of reduction are important features in hydroformylation, because the CO insertion necessary for the formation of aldehydes is reported to require small metallic cobalt sites [45, 46]. The dispersion and the extent of reduction are influenced by many factors including method of preparation, precursor used, metal loading and pretreatment conditions used. The method of preparation may have a significant influence on the dispersion achieved. The Co/SiO_2 catalysts prepared by impregnation have exhibited higher extents of reduction, higher hydrogen uptakes and higher specific activities in CO hydrogenation than their precipitated counterparts [47, 48]. Moreover, catalysts with high dispersions have been obtained with ALD where the catalyst precursor is reacted from the gas phase with the support [39].

Two different preparation methods, ALD and impregnation, and two different precursors, $Co(acac)_3$ and $Co(NO_3)_2$, have been used for the preparation of the Co/SiO_2 catalysts. The characteristics of the catalysts are shown in Table 4. The activity of the $Co(A)/SiO_2$ catalysts of varying metal content (5–16 wt%) prepared by ALD with the $Co(acac)_3$ precursor on silica was compared to the activity of the 4 wt% $Co(N)/SiO_2$ catalyst prepared by impregnation using a nitrate precursor. In addition, the effect of aluminium nitride modification of the silica support on hydroformylation activity was studied. These catalysts were prepared by reacting $Co(acac)_3$ with silica surfaced with varying degree with aluminium nitride.

Table 4. Characteristics of the Co/SiO_2 catalysts after hydrogen reduction[a]. [I, II]

Catalyst	Atmosphere	Extent of reduction[b] (%)	Total H_2 uptake (cm^3/g)	Dispersion[c] (%)	Metal particle size[c] (nm)
4-Co(N)/SiO_2	Air	84	0.55	8.5	11.3
5-Co(A)/SiO_2	Air	52	1.2	23	4.3
11-Co(A)/SiO_2	Air	54	1.9	17	5.6
16-Co(A)/SiO_2	Air	63	1.4	7.6	12.6
5-Co(A)/SiO_2[e](inert)	Inert	n.d.	1.6	17[d] (33[c])	6[d] (3[c])
5-Co/2·AlN/SiO_2[e]	Inert	n.d.	0.36	4[d]	25[d]
3-Co/6·AlN/SiO_2[e]	Inert	n.d.	0.20	3[d]	29[d]

[a] After hydrogen reduction at 550 ºC, except at 400 ºC for 4-Co(N)/SiO_2.
[b] Determined by oxygen titration.
[c] Calculated from the total H_2 uptake by using the spherical geometry assumption for cobalt particles and corrected by the extent of reduction.
[d] No correction for the extent of reduction.
[e] Silica precalcined at 750 ºC. The catalyst samples were handled inertly.
n.d. = not determined

Before hydroformylation reactions, the catalysts were pretreated in situ by hydrogen in order to reduce cobalt to Co^0. For 4-Co(N)/SiO_2, hydrogen treatment at 400 °C was adequate for the reduction of the cobalt [49]. For the removal of acac ligands and reduction of cobalt before hydroformylation reactions, the Co(A)/SiO_2 catalysts were treated by hydrogen at 550 °C. The temperature of 550 °C was chosen because Backman et al. [41] observed a maximum in the hydrogen chemisorption capacity for Co(A)/SiO_2 after hydrogen treatment at 550 °C. This pretreatment temperature was also adopted for the aluminium nitride modified Co(A)/*n*·AlN/SiO_2 catalysts. The Co/*n*·AlN/SiO_2 catalysts were handled inertly due to the moisture sensitivity of the AlN modified support.

3.1.2 Activity of Co/SiO_2 catalysts in ethene hydroformylation

The purpose of these experiments was to determine the effect of metal dispersion and extent of reduction of Co/SiO_2 catalysts on hydroformylation activity and selectivity. Moreover, the effect of preparation method on the characteristics of the cobalt catalysts was studied. The 5-$Co(A)/SiO_2$ catalyst was transferred to the reactor through air, but also inertly, in order to get a reference catalyst for the AlN/SiO_2 supported catalysts that were prepared and transferred to the reactor inertly. The activity and selectivity of the cobalt catalysts in ethene hydroformylation is presented in Figure 2. The main products were ethane, propanal and propanol. In addition, small amounts of C_6O were formed.

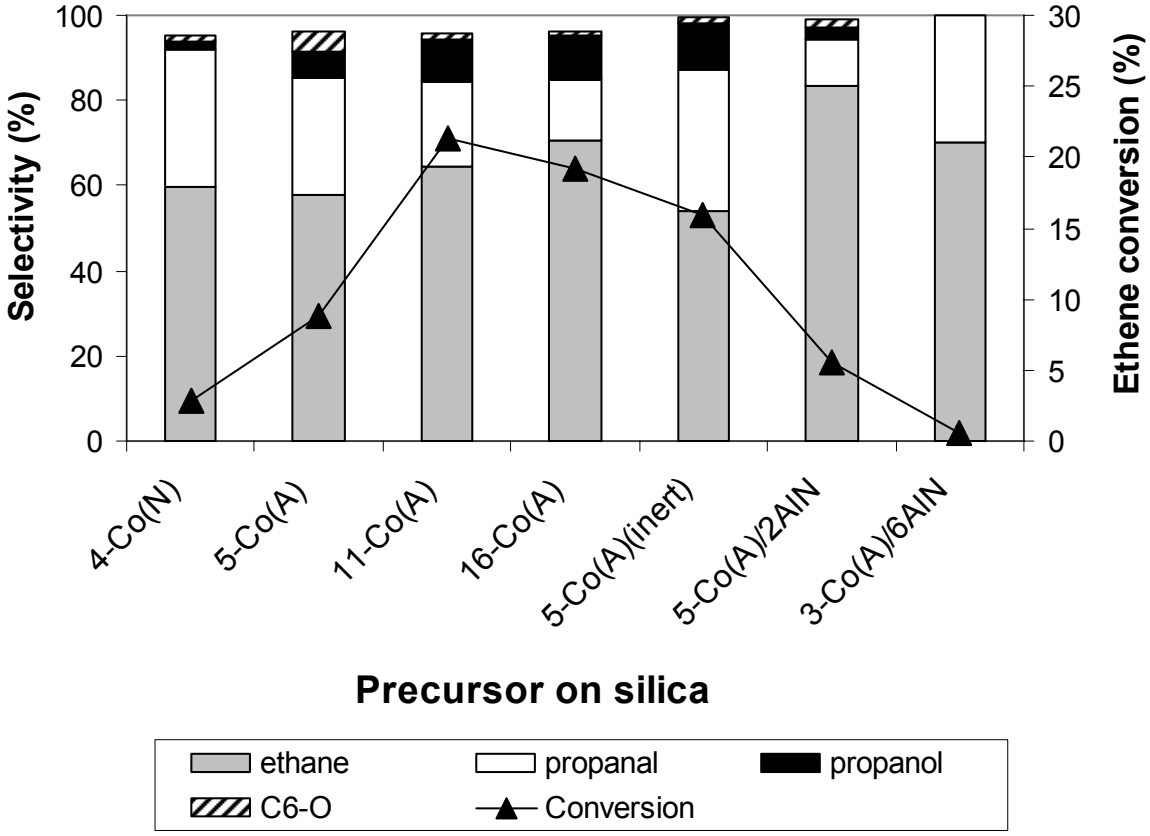

Figure 2. Ethene conversion and product selectivities for cobalt catalysts in ethene hydroformylation; T = 175 °C, p = 0.5 MPa, $Ar:CO:H_2:C_2H_4$ = 1:2:2:2 mol:mol, WHSV = 2.5 h^{-1}. [I, II]

There was a clear difference in the activity of the catalysts prepared by ALD depending on whether the catalyst was handled inertly or through air. From the 5 wt% cobalt catalysts, the best ethene conversion of 15% was obtained with the 5-Co(A)/SiO_2(inert) catalyst, compared to 9% conversion for the 5-Co(A)/SiO_2 catalyst handled in air. In accordance, the hydrogen chemisorption capacity (Table 4) was higher for the 5-Co(A)/SiO_2(inert) catalyst than for the catalyst handled in air. Also, the oxo-selectivity obtained was higher for the 5-Co(A)/SiO_2(inert) catalyst (45%) than for 5-Co(A)/SiO_2 (39%). The extent of reduction for the inertly handled Co(A)/SiO_2 catalyst could not be determined by oxygen titration due to the air and moisture sensitivity of the catalyst. If it is assumed that the extent of reduction is similar to both catalysts, the dispersion of cobalt on silica is improved by inert handling of the catalyst. These results suggest that high dispersion of cobalt is beneficial for CO insertion.

Of the 5 wt% cobalt catalysts, the impregnated 4-Co(N)/SiO_2 was the least active (X = 3%) with the lowest hydrogen uptake and consequently, the lowest dispersion (Table 4). However, the oxo-selectivity of the 4-Co(N)/SiO_2 catalyst was surprisingly high (35%) considering the low dispersion of the catalyst. The low conversion level obtained with the impregnated catalyst might have influence on the oxo-selectivity. Indeed, at a higher conversion level (X = 12%, at 193 °C and WHSV of 1.25 h^{-1}), the oxo-selectivity dropped slightly to 28%. On the other hand, the cobalt particles were almost fully reduced (84%) compared to the low extents of reduction for the Co(A)/SiO_2 catalysts, which may partly explain the higher than expected oxo-selectivity.

With increasing metal content (from 5 to 16 wt%), the oxo-selectivity of the Co(A)/SiO_2 catalysts decreased from 39 to 25%, and this decrease appeared to be related to the decreasing dispersion. Simultaneously, the selectivity towards hydrogenation products, i.e. both towards ethane and propanol, improved (Figure 2). The extents of reduction remained low for the Co(A)/SiO_2 catalysts, which is an indication of a strong support-metal interaction. Since the extent of reduction for all the Co(A)/SiO_2 catalysts was in the range 52–63 %, the effect of extent of reduction on the changes in oxo-selectivity can be excluded. Thus, these results confirm that CO insertion activity is related to the presence of small cobalt sites. One might argue that the oxo-selectivity is dependent upon the varying

conversion levels of the Co(A)/SiO_2 catalysts. However, the results of Takeuchi et al. [45] with a 5 wt% cobalt-carbonyl based Co/SiO_2 catalyst showed that the oxo-selectivity was unchanged at different conversion levels (X = 6–63 %) in the temperature range of 150–210 °C. Moreover, these results do not reveal if unreduced cobalt is active for CO insertion.

In conclusion, these results show that catalysts with higher dispersion are obtained with ALD technique using a $Co(acac)_3$ precursor than with impregnation using a cobalt nitrate precursor. Moreover, the oxo-selectivity is related to the dispersion of the cobalt metal: the higher the dispersion, i.e. the smaller the cobalt metal particles on the catalyst, the better the CO insertion activity and the oxo-selectivity.

3.1.3 Activity of Co/n·AlN/SiO_2 catalysts in ethene hydroformylation

A new type of AlN/SiO_2 support was studied in hydroformylation in order to determine the effect of a basic additive on hydroformylation activity [II]. Amines have been reported to favour the single-step formation of alcohols in hydroformylation [50] and nitride materials have been successfully used as supports in hydroformylation [51]. However, as illustrated in Figure 2, the AlN modification was not beneficial for the hydroformylation activity and selectivity. Steady-state conversion, reached after about 5 h for all the catalysts, decreased drastically with increasing AlN content of the support from 16% for pure silica-supported catalyst to 5.6% and 0.6% for the 2·AlN/SiO_2 and 6·AlN/SiO_2-supported catalysts, respectively. Moreover, the oxo-selectivity decreased from 46% for 5-Co(A)/SiO_2 to 16% for 5-Co(A)/2·AlN/SiO_2. For the 5-Co(A)/6·AlN/SiO_2, the oxo-selectivity did not decrease as drastically (S_{oxo} = 30%), but the selectivities were probably influenced by the very low conversion level and also by the detection accuracy.

The total hydrogen chemisorption capacity measured at 30 °C decreased with increasing AlN content of the support (see Table 4). It was not possible to determine the extents of reduction by oxygen titration due to the air and moisture sensitivity of the catalysts. The decreasing trend in the chemisorption capacity was partly related to the lower cobalt contents for the Co/*n*·AlN/SiO_2 catalysts (see Table 2 in [II]). However, the decrease in

hydrogen chemisorption capacity was more drastic than what would be expected on the basis of the cobalt contents alone. The explanation seems to be the increase in cobalt particle size and the corresponding decrease in dispersion. The lower dispersion on AlN/SiO_2 support than on silica support was probably due to differences in the mechanism of bonding of the cobalt reactant on the supports. On 5-$Co(A)/SiO_2$, the acac/Co ratio after the reaction of the cobalt reactant was well below two [40]. The acac/Co ratio increased with the extent of aluminium nitride modification, being two for the 5-$Co(A)/6{\cdot}AlN/SiO_2$ catalyst. The acac/Co ratio of two enabled the desorption of $Co(acac)_2$ from the surface during heating and allowed the formation of larger cobalt particles. The hydroformylation results are in agreement with the hydrogen chemisorption results. The selectivity towards oxo-products decreased with increasing AlN content, i.e. with decreasing dispersion.

3.2 Rh/C and Rh/SiO_2 catalysts

Active carbons have many features that make them suitable materials for use as catalyst supports. Carbon supports have high surface areas which, together with the pore structure, can be varied relatively easily. Also, carbon is inexpensive, inert in corrosive environments, and precious metals supported on it can be easily recovered. Moreover, active carbon has been reported to exhibit beneficial characteristics in carbonylation: it can suppress dissociative hydrogen adsorption as well as inhibit dissociative CO adsorption [52]. These characteristics are important in hydroformylation as well. The three types of activated carbon used in this study [III] were peat based Norit Rox 0.8 (N), coconut based carbon (C) from Johnson Matthey and wood based Takeda Shirasaki (T). The detailed characterisation of the supports and the catalysts has been reported elsewhere [42] as well as their catalytic activity in methanol hydrocarbonylation [53]. Since, in addition to high dispersion, the existence of partly reduced rhodium sites has been reported to be beneficial in hydroformylation, the reducibility of the Rh/C catalysts was studied in more detail by temperature programmed reduction (TPR) using hydrogen as the reducing gas. The dispersion and the extent of reduction as well as the effect of pretreatments are discussed in connection with the activity and selectivity results for ethene hydroformylation [III]. The Rh/C catalysts were compared with Rh/SiO_2 [IV].

3.2.1 Characteristics of Rh/C catalysts

The effect of characteristics of active carbon supports on the resulting Rh/C catalysts was studied in detail by Halttunen et al. [42]. They noticed that the dispersion was dependent on porosity and pH of the active carbon support and the type of oxygen-containing species present on the active carbon support. Meso- and macroporosity improved mass transfer during impregnation, and thereby, in part, increased the distribution of the metallic species within the carbon support. The amount of meso- (d_{pore} = 2 - 50 nm) and macropores (d_{pore} > 50 nm) was highest for carbon (N) (32%) and carbon (T) (15%) whereas carbon (C) was mainly microporous (d_{pore} < 2 nm) (95%).

The particle size of rhodium on active carbon was determined by TEM, XPS and hydrogen chemisorption and the results are collected in Table 5 [42]. Hydrogen chemisorption gives an average value for the particle size, but TEM provides information about the actual particle size distribution. TEM images indicated that rhodium was evenly distributed on Rh/C(T) after hydrogen reduction with a uniform particle size of 2–7 nm. On Rh/C(C) the particle size varied from 4 to 10 nm and some of the particles formed large aggregates (>10 nm). The variation of the size of the particles was greatest in the case of Rh/C(N). Some particles were < 2 nm in diameter, whereas others were about 6 nm and, to some extent, aggregated. XPS results confirmed the existence of aggregates or very small particles on Rh/C(N). In hydrogen chemisorption, the chemisorption stoichiometry for CO varies, because the species may chemisorb in the linear, bridged and subcarbonyl forms, offering a chemisorption stoichiometry of one, a half, and two or more, respectively. Thus, high CO chemisorption stoichiometry is favoured for very small particles. In agreement with the XPS results, the high CO/H ratio from the chemisorption results suggested that particles on Rh/C(N) were very small in size. According to hydrogen chemisorption, which gives only an average value for the particle size, the particle size increased in the order Rh/C(C) < Rh/C(T) < Rh/C(N). [42]

Table 5. Characteristics of Rh/C catalysts after hydrogen reduction at 400 °C [42].

	Particle size estimates (nm)		Hydrogen chemisorption	
	TEM	**XPS**	**CO/H ratio**	**Particle size[a] (nm)**
Rh/C(C)	4–10 > 10	3.3	1.4	0.95
Rh/C(N)	< 2 6 aggregates	-very small particles or aggregates	6.6 –> very small particles	1.6
Rh/C(T)	2–7	2.4	1.7	1.4

[a] Calculated from irreversible hydrogen uptakes using the 'button' or 'plate' like geometry assumption and corrected by the extent of reduction.

Since the surface of the carbon (T) was acidic (pH = 6.0), it had more active centres for the adsorption of cations (Rh^{3+}) than carbon (N), which is neutral (pH = 7.0), or carbon (C), which is basic (pH = 9.1). Accordingly, rhodium seemed to be evenly distributed on carbon (T), whereas some aggregates were present on both carbon (N) and (C). Oxygen containing sites have been reported to act as adsorption sites for the metallic species and it is both the amount and the type of oxygen groups that affect the dispersion. Halttunen et al. [42] assumed that the CO evolving groups were more important in regard to the distribution of rhodium on Rh/C, since the major part of the CO evolving groups stayed intact at the temperature of reduction (400 °C), whereas most of the CO_2 evolving groups were decomposed. Thus, the metal species adsorbed on the oxygen sites, decomposing through CO_2, mobilised rhodium during reduction. In accordance, the agglomeration of rhodium was observed for the Rh/C(N) and Rh/(C) catalysts, which exhibited a high amount of CO_2 evolving acidic groups, whereas rhodium was evenly distributed on Rh/C(T), which contained a small amount of CO_2 desorbing groups. Thus, the best dispersion after hydrogen reduction at 400 °C was obtained with carbon (T), a mesoporous carbon support which contained a high amount of thermally stable oxygen groups for bonding the active component.

3.2.2 Reducibility of Rh/C catalysts

The reducibility of the Rh/C catalysts was studied by TPR. Figure 3 shows the hydrogen consumption during TPR measurements, together with water and methane formation as a function of temperature. The hydrogen consumption during the TPR below 250 °C was mainly due to the formation of water (Figure 3A), whereas at temperatures above 250 °C the formation of methane predominated (Figure 3B). Since the determination of water and methane was not quantitative, the extents of reduction were evaluated from hydrogen consumption. The results are shown in Table 6. The characteristics of the 6-Rh/SiO_2 catalyst are included as well. The calculations had to be limited to temperatures below 250 °C since at higher temperatures methane was formed and only the formation of water results from the reduction of rhodium.

Table 6. Dispersions, particle sizes and extents of reduction for Rh/C and Rh/SiO_2 catalysts [III, IV].

Catalyst	Dispersion[a] (%)	Metal particle size[b] (nm)	H_2 consumption[c] ($mmol/g_{Rh}$)	Extent of Reduction (%)		
				TPR[d]		XPS[e]
				1st peak	1st+2nd peak	
7-Rh/C(C)	27	0.7	44.0	29	44	78
5-Rh/C(N)	4	4.3	14.2	12	39	94
7-Rh/C(T)	13	1.4	15.2	8	20	62
6-Rh/SiO_2	62	0.3	-	-	-	85[f]

[a] Calculated from irreversible hydrogen uptake and corrected by the extent of reduction after hydrogen reduction at 400 °C for 1 h for Rh/C catalysts and at 300 °C for 3 h for Rh/SiO_2.
[b] Calculated from irreversible hydrogen uptakes using the 'button' or 'plate' like geometry assumption and corrected by the extent of reduction.
[c] Total hydrogen consumption (TCD) during TPR measurement up to 400 °C.
[d] Calculated from the H_2 consumption (TCD) by fitting Gaussian curves assuming Rh^{3+} as the state of oxidized rhodium on the support: 1st peak corresponding to appr. temperatures <150 °C and 1st+2nd peak to temperatures < 250 °C.
[e] After hydrogen reduction at 400 °C for 1 h.
[f] Extent of reduction from oxygen titration.

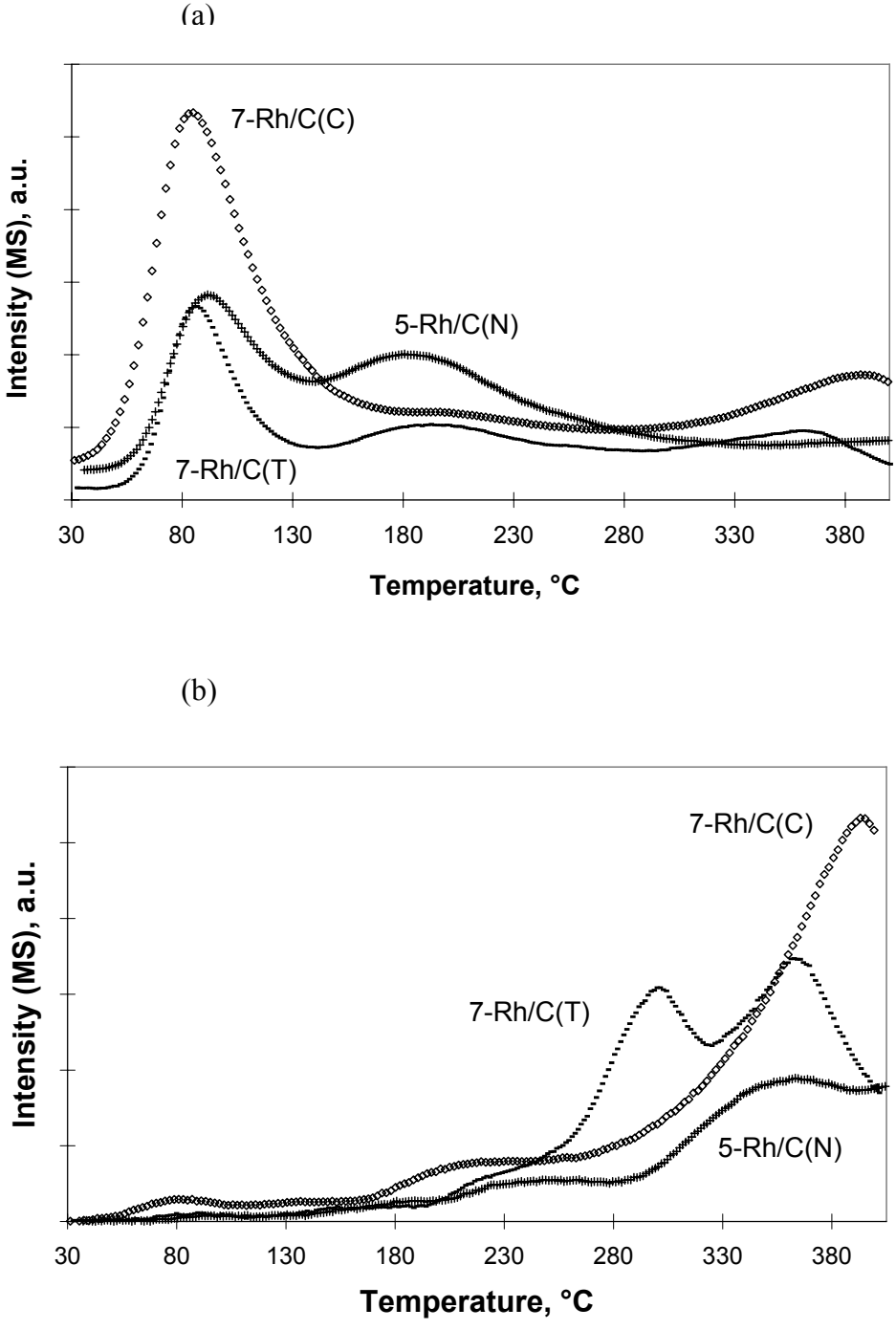

Figure 3. (a) H_2O formation (mass number 18) and (b) CH_4 formation (mass number 16) during TPR measured by MS as a function of temperature for Rh/C catalysts (a.u. = arbitrary units). [III]

The first peak maximum for hydrogen consumption was at 85–90 °C ($Rh_2O_3 + 3H_2 \rightarrow 3H_2O + 2Rh^0$). The reduction of 7-Rh/C(C) proceeded to a greater extent (29%) at a lower temperature than did the reduction of 5-Rh/C(N) and 7-Rh/C(T). At 250 °C, the extent of reduction was similar for 7-Rh/C(C) and 5-Rh/C(N) (44% and 39%), but it was much lower for 7-Rh/C(T) (20%). Thus, the TPR results show that the reduction of Rh/C started at temperatures clearly below those used for the reaction tests. For all three catalysts, the extent of reduction at 400 °C, as determined by XPS, was considerably higher than the extent of reduction at 250 °C, as determined by TPR – a result at least partly caused by the higher reduction temperature in question.

It was concluded that the high hydrogen consumption on 7-Rh/C(C), together with high methane formation, was apparently due to the rhodium catalysed support gasification, in agreement with the results of Tomita et al. [54]. This support gasification may cause agglomeration of rhodium during hydrogen pretreatment. It remained, however, unexplained why the gasification was significantly more pronounced on 7-Rh/C(C) than on 5-Rh/C(N) or 7-Rh/C(T).

In summary, the TPR experiments showed that the reduction of 7-Rh/C(C) clearly started below the temperature used for the reaction tests (173 °C) whereas for 5-Rh/C(N) and 7-Rh/C(T), higher reduction temperatures were required. Moreover, on 7-Rh/C(C) the rhodium catalysed support gasification may cause agglomeration of rhodium.

3.2.3 Catalytic activity after hydrogen reduction

Figure 4 shows catalytic activity for rhodium catalysts after different pretreatments. After hydrogen reduction at 400 °C, the highest activity and best selectivity towards propanal was obtained with the 7-Rh/C(C) catalyst. The propanal selectivity was 50% - an exceptionally high selectivity at these conditions compared to 41% for 5-Rh/C(N), 40% for 7-Rh/C(T) and 35% for 6-Rh/SiO_2. Since the presence of unreduced sites has been proposed to increase the activity for CO insertion, the performance of the catalysts was considered in terms of extent of reduction. The partly reduced catalysts, 7-Rh/C(C) and 7-Rh/C(T),

exhibited the highest conversion and highest yields of propanal. In addition to partly reduced rhodium sites, the small size of the metal is important for aldehyde formation. As indicated by the results from TEM and hydrogen chemisorption, 7-Rh/C(C) and 7-Rh/C(T) both had small particles, favourable for CO insertion. Together the XPS, TEM and chemisorption results indicated that after hydrogen reduction, both 7-Rh/C(C) and 7-Rh/C(T) had sites favourable for hydroformylation, i.e. partly reduced rhodium sites sufficiently small in size. The higher selectivity of 7-Rh/C(C) towards propanal still remained unexplained. The low hydroformylation activity of 5-Rh/C(N) was in agreement with the characterisations: according to TEM there were very small particles and large aggregates present on 5-Rh/C(N), and XPS shows they were fully reduced. The large particles were more active in hydrogenation and less active in hydroformylation. Moreover, the considerably lower overall activity of 5-Rh/C(N) was explained by the low total hydrogen uptake.

Even though the dispersion calculated from the hydrogen uptake for 6-Rh/SiO_2 was very high (62%) and thus, the particle size was small, the oxo-selectivity was lower (35%) than for the carbon supported catalysts. More information about the particle size might be obtained from the CO/H ratio as determined by chemisorption. This ratio for 6-Rh/SiO_2 was low (0.92), which does not confirm the existence of very small particles. The extent of reduction was also quite high (85%). Apparently, the fully reduced rhodium sites on 6-Rh/SiO_2 were active in hydrogenation. It is of interest that the hydrogen uptake for 6-Rh/SiO_2 was ten times higher than that for 5-Rh/C(N), but the activity still remained about the same. TEM characterisations would also be informative for the 6-Rh/SiO_2 catalyst.

SEM results suggested the presence of KCl particles on the 7-Rh/C(C) catalyst, but not on the other two carbon supported catalysts. The potassium was most probably transferred from the support matrix onto the catalyst surface during catalyst preparation (wet steps or high temperature treatments). Potassium is capable of promoting oxygenates formation in synthesis gas reaction [55], and it may have had an unintended influence on the performance of 7-Rh/C(C).

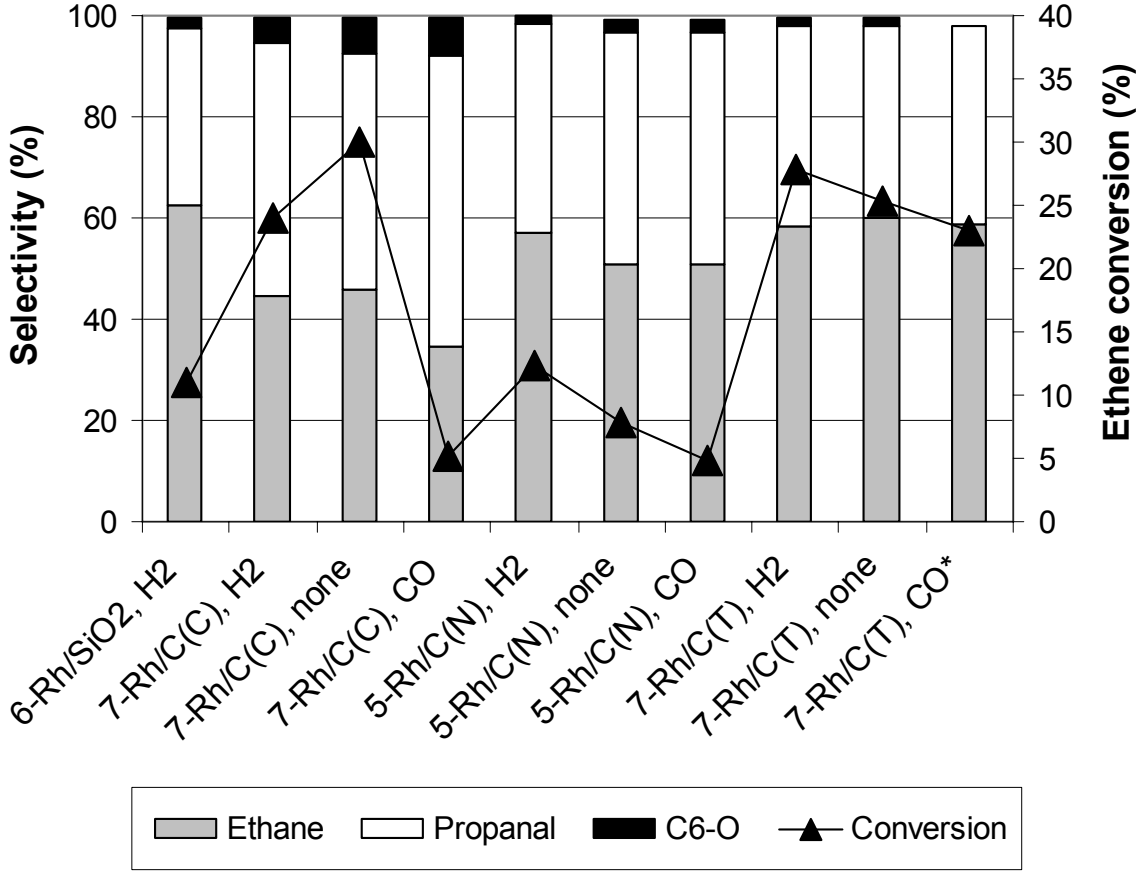

Figure 4. The product selectivities and ethene conversion for rhodium catalysts after different pretreatments; star (*) denotes CO pretreatment at 173 °C (T = 173 °C, p = 0.5 MPa, Ar:CO:H_2:C_2H_4 = 1:2:2:2 mol:mol, WHSV = 2.5 h^{-1}). [III, IV]

It is also interesting to compare these results to those for methanol hydrocarbonylation reported by Halttunen et al. [53]. The homologation reaction, producing acetaldehyde and ethanol, was favoured on 7-Rh/C(C), whereas carbonylation, producing acetic acid and methyl acetate, was favoured on 7-Rh/C(T). 5-Rh/C(N) produced both homologation and carbonylation products. The homologation reaction requires both CO insertion and hydrogenation steps similar to hydroformylation. In agreement with the hydroformylation results, 7-Rh/C(C) was also the best catalyst for homologation.

Overall, the best selectivity towards propanal was obtained with the 7-Rh/C(C) catalyst. 7-Rh/C(T) was also active, but lower selectivities towards propanal were obtained. Taken together, the XPS, TEM and chemisorption results indicated that after hydrogen reduction,

both 7-Rh/C(C) and 7-Rh/C(T), had sites favourable for hydroformylation: sufficiently small, partly reduced rhodium sites. Unintentional promotion by potassium possibly promoted the formation of oxo-products on 7-Rh/C(C).

3.2.4 Catalytic activity after carbon monoxide pretreatment or without pretreatment

To shed light on whether Rh^0 or Rh^+ is the active site for hydroformylation, the Rh/C catalysts were also tested without pretreatment [III]. The number of Rh^+ sites would be expected to be higher without any reductive pretreatment, due to lower extents of reduction. Furthermore, hydrogen reduction has been shown to induce agglomeration of rhodium on carbon [56] and, therefore, higher dispersion might be another benefit obtained by omitting the pretreatment. The performance of Rh/C was also studied by applying CO pretreatment, which has previously been found to significantly enhance the oxygenate yield on Rh/SiO_2 in CO hydrogenation via partial blockage of the active sites [57]. Such a partial blockage effect should also be beneficial for the hydroformylation catalysts. Others have claimed that CO treatment provides high dispersion [58] - another desired feature for hydroformylation catalysts.

In the absence of pretreatment, the performance of Rh/C(C) was superior to its hydrogen treated counterpart (Figure 4). Most likely, the rhodium species on the Rh/C(C) catalyst remained better dispersed in the absence of pretreatment than in conjunction with hydrogen reduction, since the undesired rhodium catalysed hydrogasification of the C(C) support was eliminated, as discussed in connection with the TPR results. In addition, the extent of reduction for Rh/C(C) was presumably lower after omitting the pretreatment, i.e. the number of unreduced rhodium sites favourable for hydroformylation was increased. However, the activity of the other two catalysts decreased slightly without pretreatment - a result apparently due to the less profound hydrogasification effect for Rh/C(T) and Rh/C(N). Also, as indicated by the TPR results, the extent of reduction for Rh/C(C) was clearly higher already at 150 ºC (29%) whereas for Rh/C(T) and Rh/C(N) it remained below 12% at this temperature. The hydroformylation reaction also requires metallic

rhodium sites for the hydrogen addition steps and it could be that the extent of reduction was too low for the other two catalysts, resulting in decrease in activity.

After high temperature CO pretreatment (400 °C) the catalyst surface was partially blocked by carbonaceous residues, which improved the CO insertion selectivity of the 7-Rh/C(C) catalyst, but suppressed the overall activity. On the other hand, low temperature CO pretreatment (175 °C) produced no benefits.

Overall, for the 7-Rh/C(C) catalyst, the best activity and selectivity was obtained without pretreatment due to better dispersed active sites and the presence of unreduced rhodium sites. However, for the Rh/C(N) and Rh/C(T) catalysts, hydrogen treatment was necessary to get enough reduced active sites. Moreover, high temperature CO pretreatment improved the CO insertion selectivity of 7-Rh/C(C), but suppressed the overall activity. Thus, the right choice of pretreatment appears to be a key factor in providing an active and selective catalyst for heterogeneous hydroformylation.

3.3 Rh/fibre catalysts

The aim was to prepare phosphine-modified catalysts in order to improve aldehyde yields, in accordance with the results from homogeneous hydroformylation processes [3]. Moreover, in propene and higher alkenes hydroformylation, formation of straight-chain aldehydes compared to branched aldehydes is improved in the presence of phosphines due to steric and electronic effects. A fibre-supported Rh-phosphine catalyst, and for comparison, a silica-supported Rh-phosphine catalyst were prepared and tested for their activity in ethene hydroformylation [IV].

The fibre-supported Rh-phosphine catalysts (Fibrecat^{TM}) were provided by former Smoptech Ltd. They have developed a method to prepare polymer supports for catalytic use by radiation grafting using high-energy electrons [43]. The pre-irradiation grafting method used minimises the formation of homopolymer and the grafted side chains are not cross-linked [59]. Moreover, polymers in different forms can be used in radiation grafting, for

example films, fibres, membranes or beads. Other benefits are the high capacity of active sites due to a high extent of grafting, and good accessibility of the active sites. In the etherification of bulky C_8 alkenes, mass-transfer over the grafted fibre catalysts was improved compared to traditional ion-exchange resin Amberlyst 35 [60].

3.3.1 Characteristics of Fibrecat™

Table 7 shows characteristics of the phosphine-containing rhodium catalysts studied in the hydroformylation of ethene [IV]. Fibrecat™ was characterised by ^{31}P NMR, using both the CPMAS and MAS methods, ^{13}C NMR and DRIFT. These characterisations were done before and after reaction, and after different pretreatments, in order to reveal the structure of the active species and the changes occurring in the active species during pretreatment and reaction. ^{31}P NMR characterisations suggested that two kinds of Rh-P species were formed on Fibrecat™ during the deposition of the $Rh(acac)(CO)_2$ precursor on the fibre support: a monophosphine species, $Rh(acac)(CO)(PS\text{-}PPh_2)$, and a bisphosphine species, $Rh(CO)_2(PS\text{-}PPh_2)_2$, as illustrated in Scheme 3.

Two different solvents, dichloromethane and acetone, were used in the preparation of Fibrecat™ in order to test whether it has effect on the distribution of the Rh-phosphine species formed. Indeed, the Rh-monophosphine/Rh-bisphosphine (mono/bis) species distribution was affected by the solvent used in the deposition stage of the rhodium precursor: with dichloromethane more bisphosphine species was formed (mono/bis = 1.5–1.8) than with rhodium deposition in acetone (mono/bis = 3.2–3.6). With higher phosphorus loading of the support (1 $mmolP/g_{support}$) the mono/bis ratio increased further to 5.6 and not all the phosphine groups reacted.

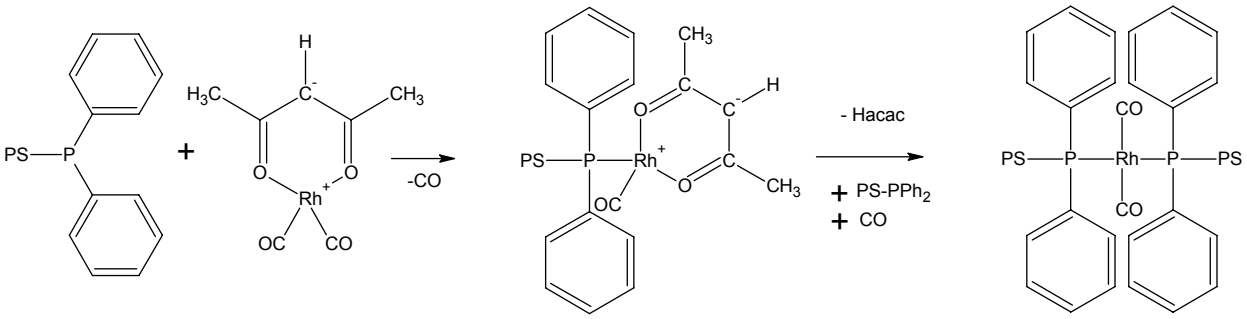

Scheme 3. Schematic presentation of Fibrecat™ preparation. [IV]

Table 7. Characteristics of the phosphine-containing rhodium catalysts [IV].

Catalyst	Rh content (wt%)	P content (wt%)[d]	S/P[e]	Rh precursor	Solvent	Mono/ bis ratio[f]
3-Fibrecat™	**2.9**[a] (4.0[b])	1.2	10	$Rh(acac)(CO)_2$	dcm	1.5
4-Fibrecat™	**4.4**[a] (6.7[b])	1.3	10	$Rh(acac)(CO)_2$	dcm	1.8
8-Fibrecat™	n.d. (7.7[b])	2.3	10	$Rh(acac)(CO)_2$	dcm	n.d.
3-Fibrecat™(Acet)	n.d. (2.8[c])	1.2	10	$Rh(acac)(CO)_2$	acetone	3.6
4-Fibrecat™(Acet)	n.d. (4.2[b])	1.2	10	$Rh(acac)(CO)_2$	acetone	3.2
6-Fibrecat™(Acet)	n.d. (5.9[c])	3.1	4	$Rh(acac)(CO)_2$	acetone	5.6
2-Rh-PPh_3/SiO_2	n.d. (2.0[d])	0.6	-	$Rh(acac)(CO)(PPh_3)$	dcm	-

[a] Method A: The catalyst is burned at 900 °C and dissolved in $HCl+Cl_2$(gas); rhodium content is determined by ICP.
[b] Method B: The catalyst is mixed with sodium peroxide and sodiumcarbonate in a Zr crucible and heated on a bunsen burner until the exothermic reaction ceases. The residue is dissolved in H_2O; rhodium content is determined by AAS.
[c] Method C: Value based on the rhodium content of solution after rhodium deposition; determined by AAS.
[d] Value given by manufacturer.
[e] Styrene/styryldiphenylphosphine molar ratio.
[f] Molar ratio of the Rh-monophosphine species to the Rh-bisphosphine species determined by ^{31}P NMR.
n.d. = not determined
dcm = dichloromethane

Figure 5 shows the fitting of the centre bands of the ^{31}P MAS NMR spectra of 4-Fibrecat^{TM} before and after CO/H_2 treatment. The pretreatments with CO or CO/H_2 converted the Rh(CO)(acac)(PS-PPh_2) species at 48.7 ppm to a new species, whose peak position was around 35 ppm (Figure 5b). From the quantitative ^{31}P NMR results it was concluded that pretreatment with CO/H_2 was more effective than pretreatment with carbon monoxide in converting the acac species to the species at 35 ppm. The bisphosphine peak at 28 ppm shifted a little to 26.5 ppm and became narrower, perhaps due to some sort of annealing of the polymer matrix. The ^{13}C CPMAS NMR spectrum of 4-Fibrecat^{TM} also confirmed that peaks due to acac ligands, at 188 ppm for the carbonyl carbon and 100 ppm for the CH carbon, disappeared during CO/H_2 pretreatment (Figure 12 in [IV]).

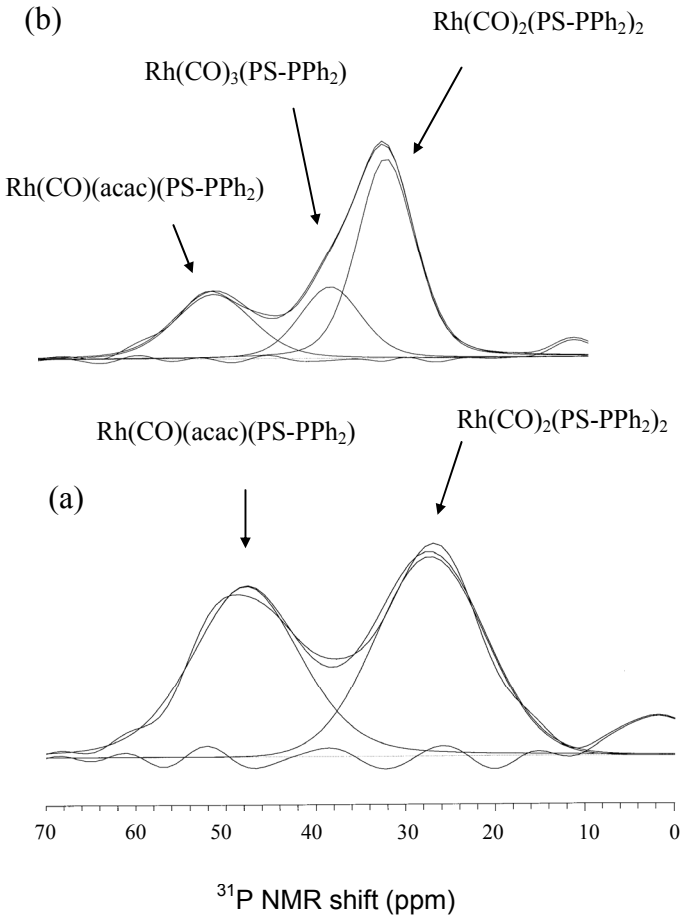

Figure 5. Fitting of the centre bands of the ^{31}P MAS NMR spectra of (a) 4-Fibrecat^{TM} (b) 4-Fibrecat^{TM} after CO/H_2 treatment at 100ºC and 0.5 MPa for 7 h. [IV]

The DRIFT spectra of 4-Fibrecat™ also provides evidence for the disappearance of acac during CO/H_2 treatment. The peaks for the acac ligand in Rh(acac)CO(PS-PPh_2) at 1580, 1518, 1391, 1270 and 1097 cm^{-1} [61, 62] disappeared almost completely upon CO/H_2 treatment (Figure 8 in [IV]). In contrast to the NMR results, no changes after carbon monoxide treatment were detected by DRIFT spectroscopy. The DRIFT results also suggested the formation of a carbonyl species after CO/H_2 treatment.

The DRIFT measurements, together with the ^{31}P NMR and ^{13}C NMR measurements suggested that the species at 35 ppm in the ^{31}P NMR spectrum formed during CO and more effectively, during CO/H_2 treatments, was $Rh(CO)_3$(PS-PPh_2). It must be noted, however, that the DRIFT and NMR measurements were carried out in air and the actual species present in CO/H_2 atmosphere is probably a carbonyl hydride species, $HRh(CO)_3$(PS-PPh_2).

In the ^{31}P MAS NMR spectrum of Fibrecat™ after reaction (Figure 6), the signal for the bisphosphine species is intact at 26.3 ppm, while the signal for Rh(CO)(acac)(PS-PPh_2) at 48.7 ppm changes into a series of overlapping peaks around 40–60 ppm. The ^{13}C CPMAS NMR spectra after reaction show no peaks for acac, but a new peak appears at 7 ppm. This peak could be either a CH_2 or CH_3 group and on this basis, it was proposed that a hydrocarbon is coordinated to rhodium. The peaks appearing during reaction at 45–58 ppm might thus be Rh(PS-PPh_2)$(CO)_{3-z}(C_xH_y)_z$ (z = 1–3) species, where the species with more coordinated hydrocarbons appears at higher frequency. DRIFT results affirm as well the formation of a carbonyl-containing species after reaction.

After the reaction, the amount of species at 35 ppm is higher with the CO and CO/H_2-treated catalysts than with the catalysts not subjected to pretreatment (see Figure 9 in IV). There are fewer species at 45–58 ppm after the hydroformylation reaction with the carbon monoxide and CO/H_2-treated catalysts than with the argon-treated or non-pretreated catalysts.

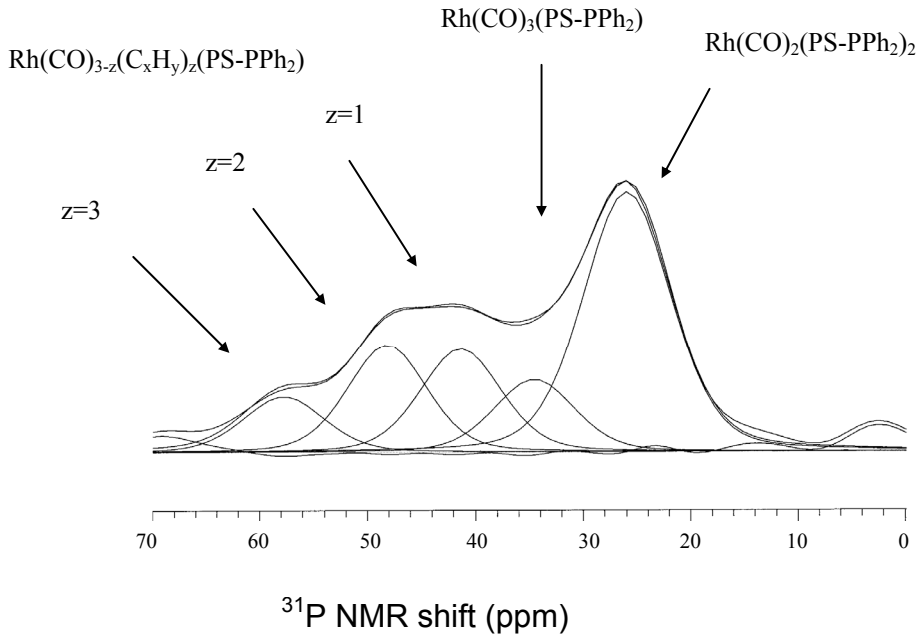

Figure 6. Fitting of the centre bands of the ^{31}P MAS NMR spectra of 4-Fibrecat™ after reaction at 110 ºC and 0.5 MPa for 46 h (no pretreatment). [IV]

In summary, ^{31}P NMR characterisations suggested that two kinds of Rh-phosphine species were formed on Fibrecat™ during the deposition of the $Rh(acac)(CO)_2$ precursor on the fibre support: a Rh-monophosphine species, $Rh(acac)(CO)(PS\text{-}PPh_2)$, and a Rh-bisphosphine species, $Rh(CO)_2(PS\text{-}PPh_2)_2$. Furthermore, the DRIFT measurements, together with the ^{31}P NMR and ^{13}C NMR measurements suggested that the Rh-monophosphine species was transformed to a $Rh(CO)_3(PS\text{-}PPh_2)$ species during CO/H_2 treatment. Moreover, hydrocarbons might be coordinated to the Rh-monophosphine species in course of the reaction.

3.3.2 Catalytic activity

8-Fibrecat™ was tested in the hydroformylation of ethene at 110 ºC and 0.5 MPa (WHSV = 2.5 h^{-1}). The main products were ethane and propanal. Small amounts of propanol, 3-pentanone, 2-methyl-2-pentenal and 2-methyl-1-pentanal (C_6-O), were also formed.

8-Fibrecat™ was very active, giving an ethene conversion of 46% and oxo-selectivity of 93%. For comparison, the activities of the unmodified rhodium catalysts were very low; ethene conversions were 1% or below. Modification of the Rh/SiO_2 catalyst with phosphine ($2\text{-}Rh\text{-}PPh_3/SiO_2$) improved the activity slightly to 1.2 %, and the oxo-selectivity was improved considerably, from 37% to 95%.

8-Fibrecat™ was tested at different reaction temperatures and pressures in order to find out limits for the use of Fibrecat™. The conversions and product yields for 8-Fibrecat™ at three different reaction temperatures are presented in Figure 7. A temperature of 135 °C was clearly too high: the catalyst deactivated from the initial 60% conversion to 10% conversion in 15 h on stream. However, it was remarkable that the excellent selectivity towards propanal was unchanged. The oxo-selectivities were 93–98% and the hydrogenation selectivities toward ethane were only 2.5–6.5% at all the temperatures and pressures tested. The temperature of 100 °C and pressure of 0.5 MPa were chosen as the reaction conditions for further studies.

There was an initial activation period of 5-10 h for Fibrecat™ at every temperature tested. Since the product selectivities did not change during the activation period, the activation period indicated change in the number of active sites. The effect of the reacting gases on the activation period was investigated by pretreatments with carbon monoxide, hydrogen and a combination of these at 100 ºC and 0.5 MPa. The effect of temperature was studied by pretreatment with argon. As illustrated in Figure 8, the argon, carbon monoxide and hydrogen pretreatments did not shorten the activation period. After CO/H_2 pretreatment, however, the conversion was already 13% after 20 minutes and the steady-state conversion was lower (about 18%) than with the other treatments (20%). A similar trend was observed at 110 °C for 8-Fibrecat™ with carbon monoxide pretreatment alone (not shown): relative to the untreated catalyst, the carbon monoxide pretreatment shortened the activation period from 15 hours to 5 hours and the conversion level decreased from 45% to 33%.

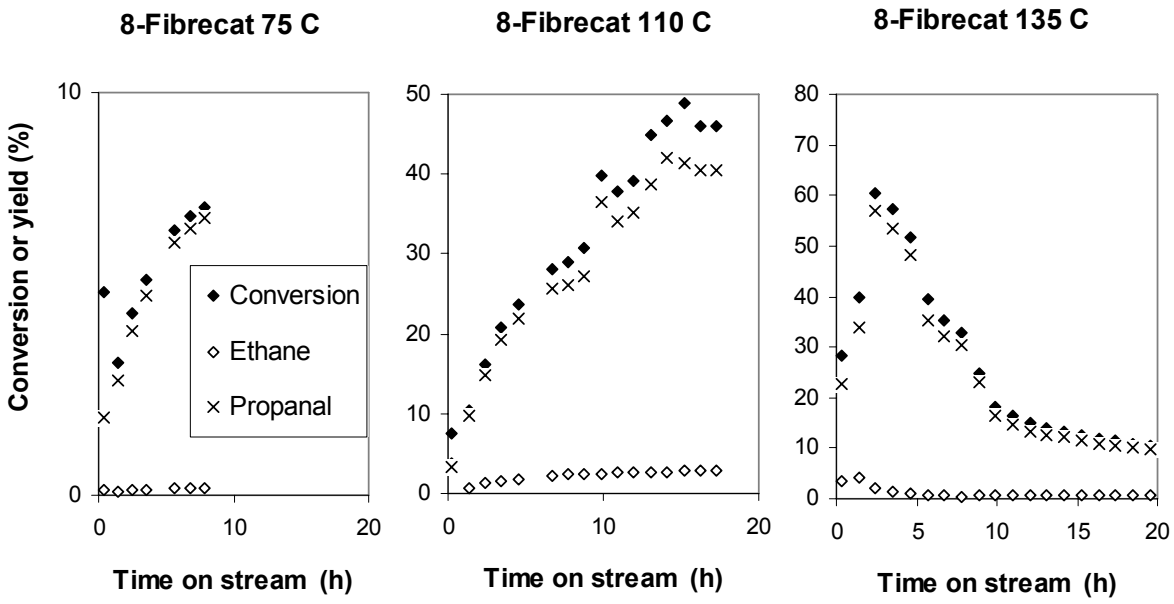

Figure 7. Ethene conversion and product yields with time for 8-Fibrecat™ at 75 °C–135 °C and 0.5 MPa; WHSV = 2.5 h^{-1}, Ar:CO:H_2:C_2H_4 = 1:2:2:2 mol:mol. [IV]

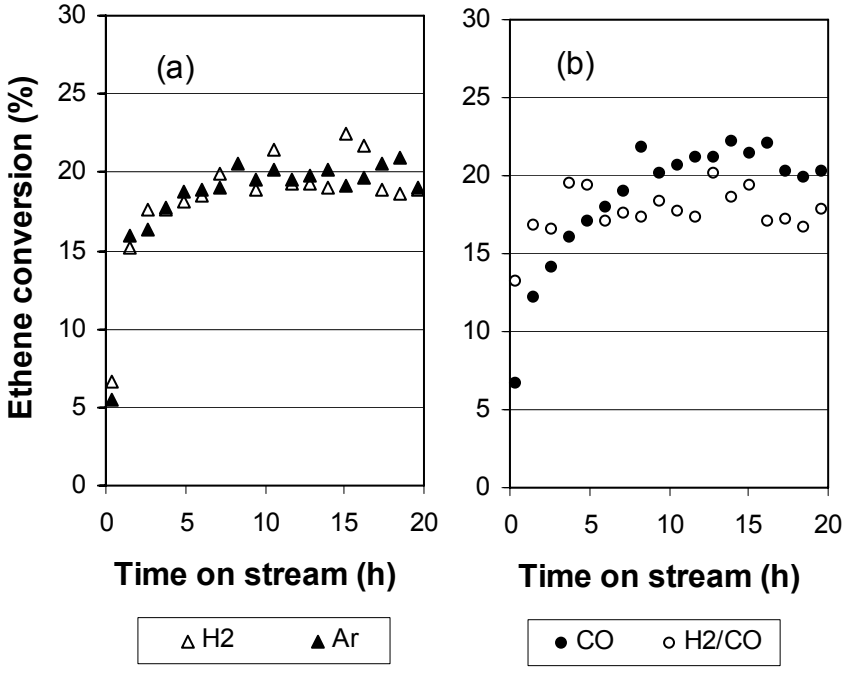

Figure 8. Ethene conversion for 3-Fibrecat™ at 100 °C and 0.5 MPa after pretreatment with (a) Ar or H_2 for 7 h and (b) CO or CO/H_2 for 7 h at the reaction temperature; WHSV = 5 h^{-1}, Ar:CO:H_2:C_2H_4 = 1:2:2:2 mol:mol. [IV]

In summary, Fibrecat™ was a promising catalyst for ethene hydroformylation: high propanal selectivity (95%) and high activity were obtained under the mild reaction conditions of 100 ºC and 0.5 MPa. At 110 °C, the pretreatment with carbon monoxide and at 100 °C the pretreatment with CO/H_2, shortened the activation period. The accompanying effect, unfortunately, was a decreased conversion level. It must be noted that the propanal selectivity remained at 95-96% during the activation period, which suggests that only the number of the active sites was changing.

3.3.3 Active species

The mechanism of the hydroformylation reaction was considered in order to relate the changes observed in the catalyst structure to the activity results. In the Rh/PPh_3-catalysed homogeneous hydroformylation, according to the widely accepted Wilkinson's dissociative mechanism [1, 2, 31], the active species are the 16-electron hydrides, $HRh(CO)(PPh_3)_2$ and $HRh(CO)_2(PPh_3)$, which are formed by the dissociation of CO from the 18-electron carbonyl hydrides (see Scheme 2).

As discussed above, once in contact with carbon monoxide, the monophosphine species $Rh(CO)(acac)(PS\text{-}PPh_2)$ was transformed to a Rh-carbonyl species, $Rh(CO)_3(PS\text{-}PPh_2)$, that is a direct catalyst precursor in hydroformylation. In a similar way, the $2\text{-}Rh\text{-}PPh_3/SiO_2$ catalyst prepared from a $Rh(CO)(acac)(PPh_3)$ precursor needs to lose the acac group before the catalyst becomes active. The activation of the bisphosphine species is simpler: all that is required is formation of the carbonyl hydride species, $HRh(CO)_2(PS\text{-}PPh_2)_2$. Accordingly, an increase in activity with time occurred only for the phosphine containing catalysts, Fibrecat™ and $2\text{-}Rh\text{-}PPh_3/SiO_2$, while the activity of the supported non-phosphine modified rhodium catalysts decreased. The activation period on Fibrecat™ could be shortened by carbon monoxide or CO/H_2 pretreatments since the catalytic precursor sites were formed already during the pretreatment. The treatment with CO/H_2 thus promotes the formation of an active species at 35 ppm and prevents the formation of the hydrocarbon coordinated $Rh(PS\text{-}PPh_2)(CO)_{3-z}(C_xH_y)_z$ (z = 1–3) species, which is less active in hydroformylation.

The activation behaviour of the catalysts prepared with acetone was similar to that of the catalysts prepared with dichloromethane, except that the activation took longer for 6-Fibrecat^{TM}(Acet) than for 3-Fibrecat^{TM}(dcm) with a similar conversion level (Fig. 4 in [IV]). This indicates that the activation of the Rh-monophosphine species was slower compared to the Rh-bisphosphine species. Moreover, the samples prepared with acetone exhibited different propanal selectivities depending on the metal loading and the mono/bis ratio: the propanal selectivity was 95% for 3-Fibrecat^{TM}(Acet) (mono/bis = 3.6), but from 91–93% for 6-Fibrecat^{TM}(Acet) (mono/bis = 5.6). Thus, the Rh-bisphosphine species appears to be more selective in producing propanal than the Rh-monophosphine species.

3.3.4 Catalyst deactivation

Hydroformylation runs lasting 50 h were carried out to assess the long-term stability of Fibrecat^{TM}. The conversion for 4-Fibrecat^{TM} decreased from 15% to 10% over a 50 h time period at 100 °C and 0.5 MPa (Figure 9). The propanal selectivity increased slightly, from 94% to 96%. At 110 ºC and 0.5 MPa, the deactivation was even more drastic with 4-Fibrecat^{TM}: conversion decreased from 28% to 10% over 40 h on stream whereas with 6.7-Fibrecat^{TM} the decrease was only 8 %.

The two main deactivation mechanisms in homogeneous hydroformylation are the degradation of the phosphine ligands and the oxidation of the phosphine ligands to phosphine oxide [63]. Degradation of the phosphine ligands is not likely under the mild reaction conditions used. Also, the quantitative ^{31}P NMR did not show a loss of phosphorus even after 50 h of reaction. The formation of Rh-dimers observed in homogeneous processes can be prevented by immobilisation of the catalyst on a support [63] and is therefore not likely on Fibrecat^{TM}.

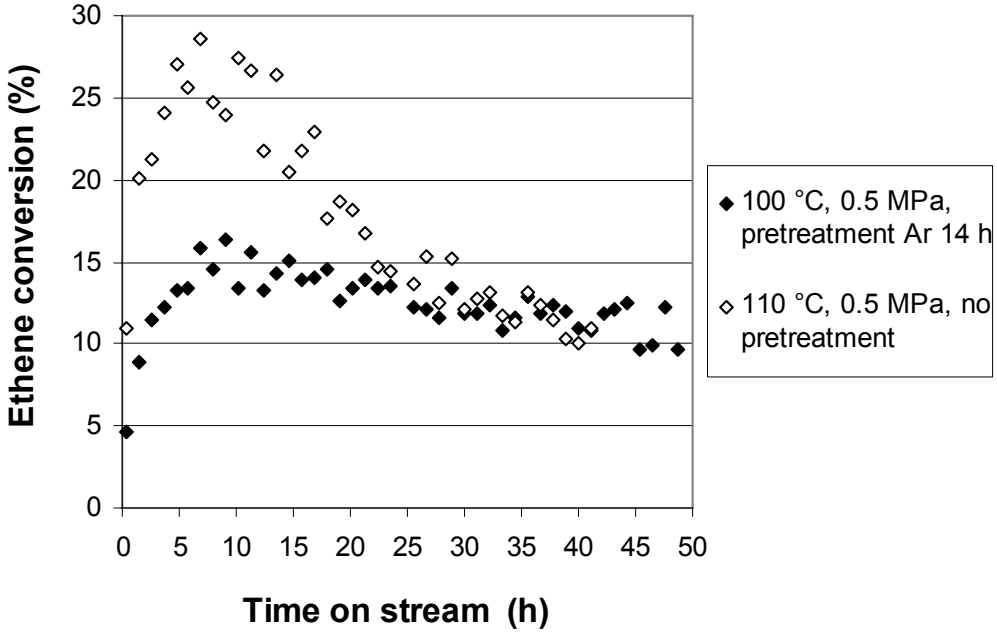

Figure 9. Ethene conversion and yields for 4-Fibrecat™ at 110 or 100 °C and 0.5 MPa; WHSV = 5 h^{-1}, Ar:CO:H_2:C_2H_4 = 1:2:2:2 mol:mol. [IV]

There might have been traces of oxygen present in the system when the reaction was started, so one should consider the possibility of oxidation of phosphine resulting in breakage of the Rh-P bond. However, examination of the ^{31}P NMR spectra shows that the ratio of the two different relaxation time components for the peak at 28 ppm, before and after CO/H_2 treatment, does not change significantly. We have assumed that the minority, faster relaxing component comes from phosphine oxide in the catalyst. If this is valid then it is reasonable to assume that there is no phosphine oxide formed during the reaction either. Moreover, the quantitative ^{31}P NMR results show that there was no loss of coordinated rhodium or phosphorus during the pretreatments or reaction.

After the initial activation period, and after reaching steady-state, the activity of Fibrecat™ decreased slightly with time. The ^{31}P NMR spectra of Fibrecat™ after the reaction showed new peaks at around 40–60 ppm and these were assigned to $Rh(CO)_{3-z}(C_xH_y)_z(PS\text{-}PPh_2)$ (z=1–3) species. These complexes were formed after both 24 h and 50 h on stream, but the amount of the species with higher z increased with time. The amount of hydrocarbon coordination was also higher at 110 ºC than at 100 ºC. As a result of coordination of two or

three hydrocarbons, there are not enough coordination sites on the catalyst for carbonyl, hydrogen and ethene (step 2 in Scheme 2) and thus the number of active sites available for hydroformylation decreases. The increased coordination of hydrocarbon with time at least partly explains the decrease in activity.

One possibility for the identity of the coordinated species would be the ethyl group, since ethyl coordination to rhodium is part of the catalytic cycle (Scheme 2), even though it should be further hydroformylated to propanal or hydrogenated to ethane. Other possible hydrocarbons are reaction products, or parts of the acetyl acetonate group, which might have decomposed in contact with CO/H_2 [64].

The deactivation was clearer at 110 ºC than at 100 ºC. Samples were exposed to temperatures just around the melting point of polyethene for a long time and then cooled fairly slowly and this could have caused annealing of the sample [65]. The possible annealing was studied by examining the CH_2 carbon region around 33 ppm in the ^{13}C NMR spectra to get a qualitative idea of the degree of crystallinity of the polyethene. No annealing was observed in 3-Fibrecat™ after CO/H_2 treatment at 100 ºC. After reaction at 110 ºC and 0.5 MPa, however, the crystallinity of the catalyst increased, indicating that some annealing of the fibres had occurred during the reaction. Thus, annealing could also be another contributing factor to the clearer deactivation of Fibrecat™ at 110 ºC compared to 100 ºC. The increase in crystallinity makes active sites in the amorphous phase less accessible for the reactants, resulting in a decrease in activity. As discussed above, the amount of hydrocarbon coordination with $z = 2$ or 3 was also higher, contributing to the deactivation at 110 ºC. One should also remember that, at the low temperature employed, some of the products, especially C_6O, even though formed in small quantities, may over time accumulate on the support of the catalyst and block part of the active sites.

In summary, the catalytic results and characterisations indicated that deactivation on Fibrecat™ was caused by formation of inactive Rh-species by hydrocarbon coordination, annealing of the polyethene support at 110 ºC and higher temperatures, and possibly by accumulation of reaction products on the surface with time. The amount of phosphorus or coordinated rhodium did not decrease during the reaction.

4 HYDROFORMYLATION OF PROPENE

To extend my findings to other alkenes, preliminary reaction tests with 3-Fibrecat™ and Rh/C were carried out in vapour-phase hydroformylation of propene (unpublished data). In propene hydroformylation, it is possible to see the capability of the catalysts to form straight-chain or branched aldehydes. Table 9 shows the activity of the rhodium catalysts in propene hydroformylation at 90–150 °C.

Table 8. Propene hydroformylation with rhodium catalysts[a].

Catalyst	Reaction conditions (°C, MPa)	Time (h)	Propene conv. (%)	Selectivities (%)			
				Propane	i-butanal	n-butanal	n/i
3-Fibrecat™	90, 0.6	11–14	3.2	3.8	42.5	53.7	1.26
3-Fibrecat™	100, 0.3	11–14	1.1	10.1	40.2	49.7	1.24
7-Rh/C(T)	150, 0.6	11–14	2.1	61.1	12.5	26.4	2.11
5-Rh/C(N)	150, 0.6	6	0.7	66.8	14.5	18.7	1.30

[a] $Ar:CO:H_2:C_3H_6$ = 4:1:1:1 mol:mol, WHSV = 3.4 h^{-1}.

Propene was much less reactive than ethene at similar reaction conditions. Propene conversion with 3-Fibrecat™ was only 3% at 90 °C and 0.6 MPa, but very high butanal selectivity was obtained (96%) with normal to branched ratio of 1.26. In order to increase conversion level, higher temperatures or pressures should be used. Since the maximum reaction temperature for Fibrecat™ is about 100 °C as revealed by the ethene hydroformylation results, reaction pressure should be increased in order to increase conversion level. 7-Rh/C(T) catalyst was the most promising catalyst in terms of the formation of the straight-chain products (n/i ratio = 2.1).

For comparison, in the studies of Reinius [5], in liquid-phase hydroformylation of propene at 100 °C and 1.0 MPa with a homogeneous catalyst, the n/i ratio was about 1.8. Moreover,

with a macroreticular-type phosphinated PS/DVB as a support, the n/i ratio was 1.23 at 100 °C and 1.4 MPa, with a conversion level of 5%, which is similar to our results. Thus, the activity of 3-Fibrecat^{TM} is indeed quite high considering the low reaction pressure used. As for ethene hydroformylation, the activity of 3-Fibrecat^{TM} increased with time.

In all, high butanal selectivity (96%) was obtained with Fibrecat^{TM} in vapour-phase hydroformylation of propene. From the carbon supported catalysts, 7-Rh/C(T) was the most promising catalyst in directing the selectivity towards straight-chain aldehydes: the normal to branched ratio was 2.1.

5 HYDROFORMYLATION OF 1-HEXENE

5.1 Activity of rhodium catalysts in 1-hexene hydroformylation

In the liquid-phase hydroformylation of 1-hexene at 150 ºC and 7.3 MPa (initial pressure), the effect of support on the performance of the Rh/C catalysts was determined. Figure 10 shows the activity of the carbon supported rhodium catalysts and a homogeneous rhodium nitrate in 1-hexene hydroformylation. The normal to branched ratio (n/i) was between 0.5–0.6 for C_7 aldehydes and between 0.7–0.9 for C_7 alcohols. The quite low n/i ratios (below 1) can be explained by the rather high reaction temperature, 150 ºC, and the rather low CO pressure. The isomerisation activity was affected by the reaction conditions rather than the Rh/C catalysts used, because selectivity towards 2-ethyl-hexanal, which is formed from 2- or 3-hexene, was 13–14% for all the rhodium catalysts tested.

At best, the activity of the solid catalysts was similar to their homogeneous counterparts. On $Rh(NO_3)_3$, the selectivity towards C_7 alcohols was remarkably higher than that of Rh/C catalysts, even at similar conversion levels. Moreover, the greatest difference between homogeneous and heterogeneous reaction was the formation of secondary products by condensation or acetalisation on the solid rhodium catalysts. These C_{14} and C_{21} products were only formed in traces on $Rh(NO_3)_3$.

Acetal formation, i.e. addition of two alcohol molecules to an aldehyde, is catalysed by a trace of strong acid [66]. This is why the acetal formation was studied in relation to the nature of the active carbon supports in more detail. The acid catalyzed formation of dimethylether decreases in gas-phase methanol hydrocarbonylation in the order Rh/C(C) > Rh/C(N) >> Rh/C(T) [53], i.e. the acidic character of the supports decreases in the same order. Since for the carbon (N) the formation of C_{21} was greatest, it was apparently the high fraction of meso and macro pores (allowing good mass transfer), together with the acidity, that was responsible for the formation of C_{21} acetals on Rh/C(N). The formation of traces of C_{21} acetals on homogeneous rhodium is explained by the good alcohol selectivity.

The activity of the Rh/C catalysts appeared to correlate with the support: the larger the pores, the better the mass transfer and the higher the activity. For the most active catalyst, Rh/C(N), 30% of the pores were larger than 2 nm in diameter compared to 15% for Rh/C(T) and 9% for Rh/C(C). Also, C_{21} acetals were only formed on a support with large enough pores – an indication of the heterogeneous functionality of the catalysts. For comparison, in the studies of Zhang et al. [67] with Co/SiO_2 catalysts, the best activity and selectivity in 1-hexene hydroformylation was obtained with average pore diameters of 6 and 10 nm.

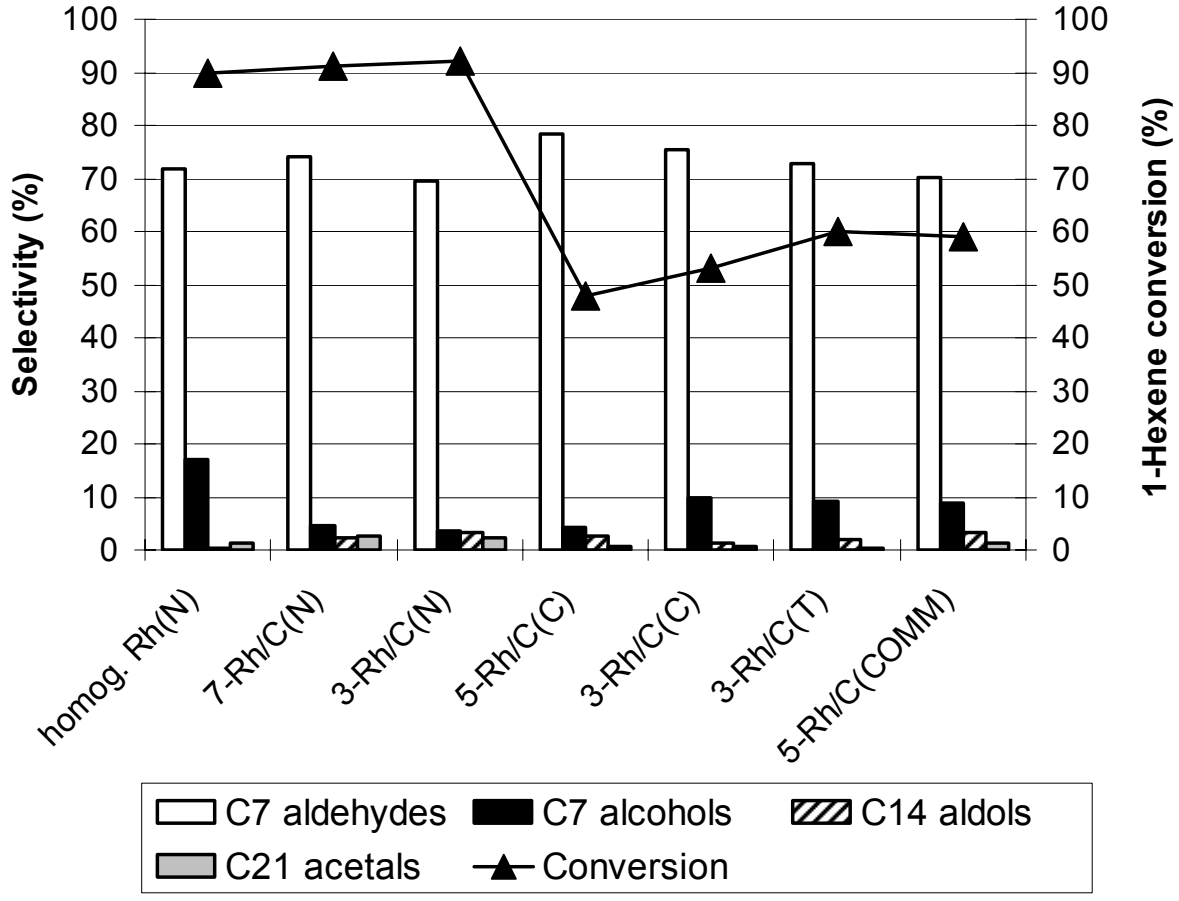

Figure 10. Conversion and selectivity for rhodium catalysts in 1-hexene hydroformylation at 150 °C and 7.3 MPa (initial pressure) after 4 h. [V]

5.2 Activity of cobalt catalysts in 1-hexene hydroformylation

The activity of nitrate and carbonyl based silica supported cobalt catalysts was compared to homogeneous cobalt nitrate and cobalt carbonyl [V]. Cobalt catalysts of carbonyl origin were chosen for study, because higher dispersions have been obtained with carbonyl based catalysts compared to nitrate based catalysts [68]. Figure 11 shows the activity of the cobalt catalysts in 1-hexene hydroformylation.

Homogeneous $Co_2(CO)_8$ was extremely active in hydroformylation; the conversion of 1-hexene to products was 96 %, whereas it was only 73 % for homogeneous cobalt nitrate. Since the solubility of $Co(NO_3)_2$ in the reaction medium was low, and cobalt nitrate has to be first transformed to $Co_2(CO)_8$ and then further to the active $HCo(CO)_4$ species, the formation of active species takes place more readily from $Co_2(CO)_8$. Also, there were differences in the selectivity: the hydrogenation to alcohols was initially higher for $Co_2(CO)_8$, but the alcohols reacted further to acetals. Since the acetal formation is catalysed by a trace of strong acid [66], the high selectivity towards acetals is not surprising considering the strong acidic character of $HCo(CO)_4$. Thus, the high selectivity towards alcohols and the strong acidic character of $HCo(CO)_4$ both affected the formation of C_{21} acetals on homogeneous $Co_2(CO)_8$.

At best, the activity of the 5-Co(N)/SiO_2 and 2Co(CO)(p)/SiO_2 catalysts was comparable to the homogeneous nitrate precursor, whereas the activities of the other catalysts were clearly lower (Figure 11). The excellent result with 2Co(CO)(p)/SiO_2 catalyst could not, however, be reproduced; problems were encountered in the catalyst preparation and handling procedure due to the air-sensitive nature of the carbonyl precursors. Another reason for lack of reproducibility might be the uncontrolled equilibrium between catalyst precursor and the dissolved active species: the reaction conditions used (CO pressure < 3.6 MPa, 150 ºC) were milder than those reported in the literature necessary to keep cobalt carbonyl species stable in solution (more than 4 MPa at 150 ºC [31]). As a result, it was very difficult to determine the effect of the cobalt precursor on the activity of the Co/SiO_2 catalysts. For rhodium, the reaction conditions needed to keep rhodium carbonyl stable in solution are noticeably milder and in fact, the experiments were repeatable from run to run.

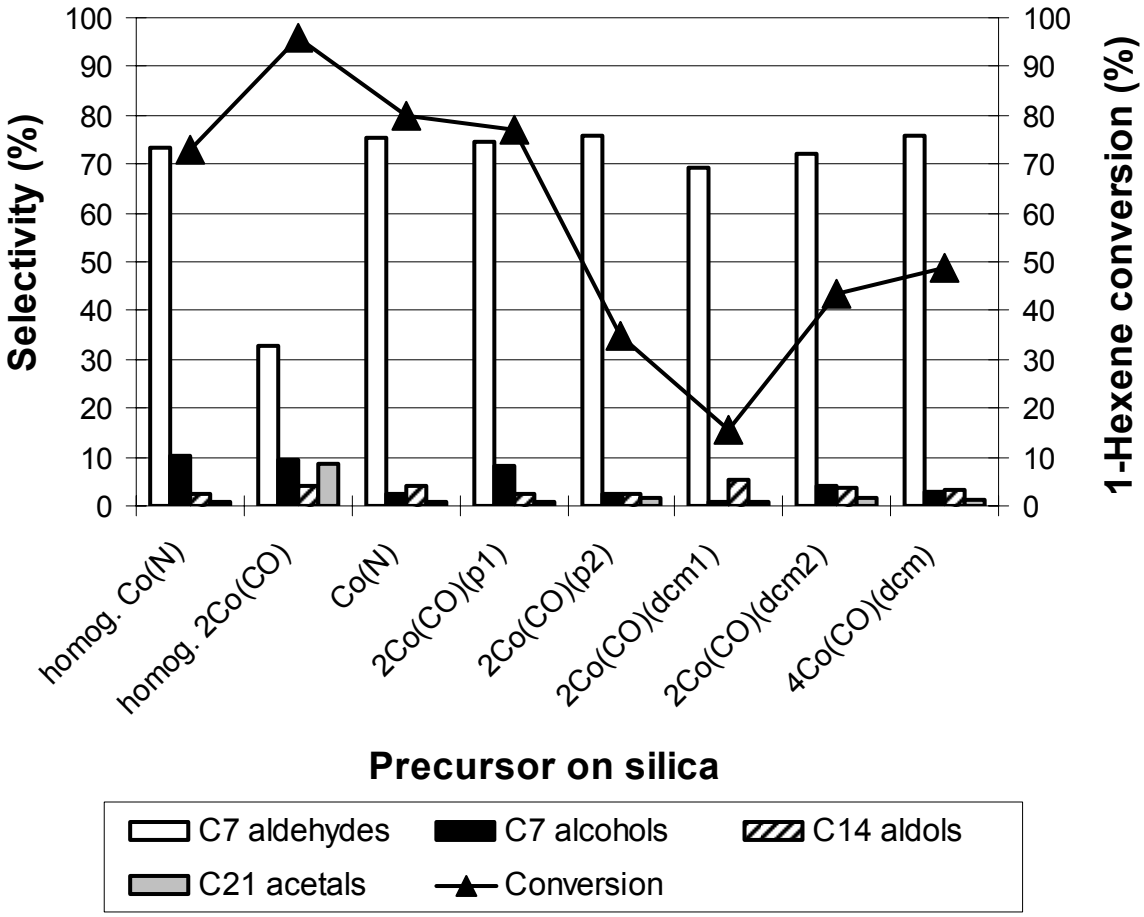

Figure 11. Conversion and selectivity for cobalt catalysts in 1-hexene hydroformylation at 150 °C and 7.3 MPa (initial pressure) after 4 h. [V]

6 STABILITY OF THE RHODIUM AND COBALT CATALYSTS IN HYDROFORMYLATION

Even though there are many reports of applying solid catalysts for heterogeneous hydroformylation, stability data is often missing. However, for industrial applications, stability of the catalysts is vital for the economics of the processes, due to the high cost of rhodium. Therefore, determination of the stability of the catalysts was an important part of this work, both in gas and liquid-phase conditions. The performance of the catalysts was evaluated as a function of time. Moreover, the stability of the solid catalysts was determined by metal analyses before and after the hydroformylation reaction.

6.1 Gas-phase hydroformylation

Under gas-phase conditions, the metal losses were less than 10% for Rh/C(N), whereas for Rh/C(T) and Rh/C(C) they were 20-30%. This could also be seen by decrease in activity with time on stream (Figure 12). Thus, the Rh/C(C) and Rh/C(T) catalysts active in the formation of propanal lost more metal than the less active Rh/C(N). Under the reaction conditions, it is possible that the supported rhodium species might form volatile carbonyls that are transported away from the support with the product flow. To confirm this assumption, a test was performed on Rh/C(C) in the absence of carbon monoxide (ethene hydrogenation): the losses were only 8%. Thus, most of the losses were due to the action of carbon monoxide on rhodium.

The stability of the catalytic performance was evaluated for 68 h on the 5-Co(A)/SiO_2 catalyst (see Figure 3 in [1]). The conversion increased from 10 to 13% over 10 h and remained almost constant thereafter, and the selectivities also remained unchanged. The increase in conversion was also observed with the 11-Co(A)/SiO_2 catalyst (again, over 10 h on stream) but not with 16-Co(A)/SiO_2 or 4-Co(N)/SiO_2, which both maintained the same activity throughout the experiment. No time dependent change in the activity on any of the

$Co(A)/SiO_2$ catalysts was detected during 1 h on stream in toluene hydrogenation [32]. Thus, it seems appropriate to assume that hydrogen did not induce the change.

The steady or increasing activity of the cobalt catalysts with time indicates that the active metal is not leached or sublimed from the support, and the stability of the catalysts was also confirmed by the metal analyses (see Table 2 in Paper [I]). The results clearly indicated that no metal was lost from the support, since the values before and after reaction were the same within the accuracy of the analyses.

Thus, the stability of the solid catalysts in heterogeneous hydroformylation is dependent on the metal in question and the reaction conditions used. As expected, the stability of the catalysts was better in gas phase [I, III] than in liquid phase [V]. The cobalt catalysts were stable at 173 ºC and 0.5 MPa, whereas rhodium losses occurred under these conditions. This difference was due to the different tendencies to form volatile metal carbonyls. $Rh(CO)_2(acac)$ and related complexes are excellent precursors for plasma enhanced deposition due to their high volatility [69-71].

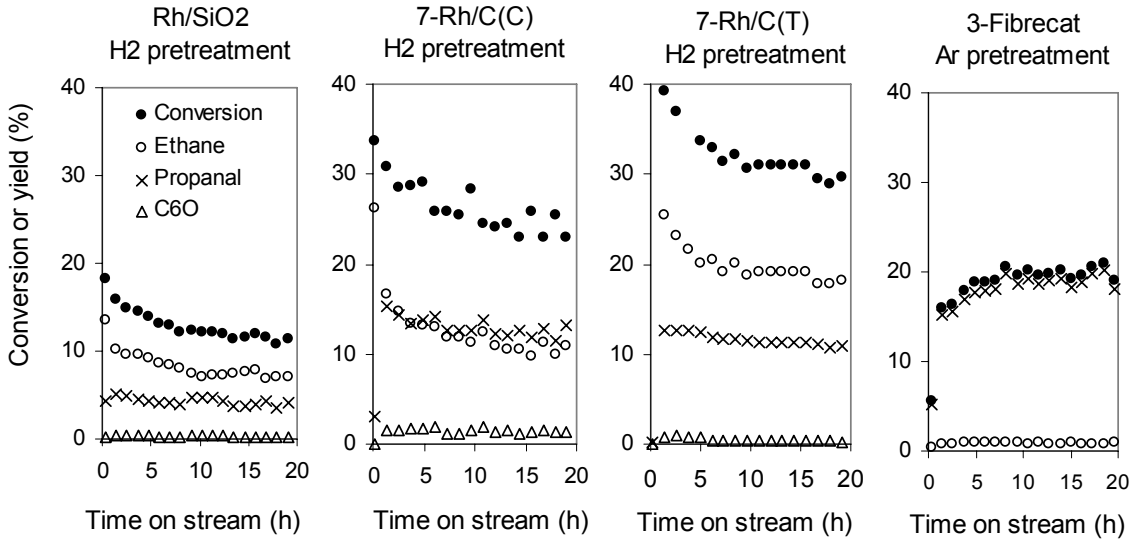

Figure 12. Ethene conversion and products yields with time for rhodium catalysts. Reaction conditions were 173 °C and 0.5 MPa (WHSV = 2.5 h^{-1}) except with 3-Fibrecat™ 100 °C and 0.5 MPa (WHSV = 5 h^{-1}); $Ar:CO:H_2:C_2H_4$ = 1:2:2:2 mol:mol.

The reaction temperature used for Fibrecat™ was much lower (100–110 ºC) than that used for unmodified rhodium catalysts, which prevented the formation of volatile carbonyls. This was confirmed by quantitative ^{31}P NMR characterisations, according to which the amount of phosphorus or phosphorus-coordinated rhodium did not decrease during the reaction. The catalytic results and characterisations indicated that deactivation on Fibrecat™ was due to formation of inactive Rh-species by hydrocarbon coordination, annealing of the polyethene support at 110 ºC, and possibly by accumulation of reaction products on the surface with time. The amount of phosphorus or coordinated rhodium did not decrease during the reaction.

6.2 Liquid-phase hydroformylation

In the liquid-phase hydroformylation of 1-hexene, the metal analyses of the catalysts before and after the reaction showed that some metal was dissolved from the support during the reaction. The losses were 20-40% of the amount deposited on the support for Rh/C catalysts and 40-50% for Co/SiO_2 catalysts. The activity of the solid catalysts was, however, not directly related to the amount of dissolved metal. The differences between the solid catalysts might be due to the different abilities to form the active carbonyl species, in the same way as was observed for homogeneous $Co_2(CO)_8$ and $Co(NO_3)_2$. Thus, the metal particle size, and therefore the strength of the metal-support or metal-metal bond, might have an influence on the ease of carbonyl formation. However, the amount of metal dissolved was not directly related to the metal dispersion. In addition, the pore size distribution of the supports influences the mass transfer of the reactants and products, and thereby also has an effect on the dissolution of the metal from the support. Accordingly, the activity of Rh/C appeared to correlate with the support, i.e. the larger the pores, the better the mass transfer of the reactants and products, and the higher the activity (see Figure 3 in paper [V]). The experiments in nitrogen or hydrogen atmospheres also resulted in metal losses, thus indicating that, in addition to synthesis gas mediated formation of active species, dissolution of the metals by product occurred.

7 CONCLUDING REMARKS

The purpose of this research was to develop a solid catalyst for heterogeneous hydroformylation. Different supports, precursors, preparation methods and pretreatments were applied in order to obtain an active, selective and stable hydroformylation catalyst.

The support characteristics and the different pretreatments had a clear effect on the dispersion and the extent of reduction and, thereby, on the activity and selectivity of the Rh/C catalysts in ethene hydroformylation. Dispersed sites were essential for hydroformylation activity, and the presence of unreduced rhodium was favourable for propanal formation. It is important to be aware that the impurities of the support matrix may promote catalysis as was the case with the unintentional promotion by potassium on 7-Rh/C(C). Also, it was evident that hydrogen chemisorption only offers an average estimate for the particle size of the metal, and that other characterisation methods like TEM and XPS are necessary in order to get a more detailed view of the rhodium distribution on the catalyst surface.

Atomic layer deposition was a good technique for the preparation of dispersed Co/SiO_2 catalysts using a $Co(acac)_3$ precursor, and a clear relation between metal dispersion and hydroformylation activity was obtained. The high metal support interaction was evidenced by quite low extents of reduction (50 %). It would be interesting to apply this technique to the preparation of rhodium catalysts as well.

The most promising rhodium catalyst in ethene hydroformylation was the fibrous polymer-supported Rh-phosphine catalyst, Fibrecat^{TM}, prepared from a $Rh(acac)(CO)_2$ precursor: high propanal selectivity (95%) and high activity were obtained under mild reaction conditions. The solvent used in the impregnation step had an effect on the Rh-monophosphine/Rh-bisphosphine species distribution on Fibrecat^{TM}. More research is needed to further study the effect of the preparation conditions on the catalyst structure and the activity of the Rh-monophosphine and Rh-bisphosphine species in hydroformylation.

In industrial heterogeneous hydroformylation, the stability of the catalysts is essential to the economics of the process. Therefore, the determination of the stability of the catalysts was an important part of this work as well. Clearly, the stability of the catalysts was related to their capability to form volatile or soluble carbonyls and thus, directly related to the reaction conditions applied. A careful consideration of the reaction conditions versus properties of the catalytic metal and the support matrix are essential to obtain a stable solid catalyst for heterogeneous hydroformylation.

8 REFERENCES

1. Breit, B. and Seiche, W., Recent advances on chemo-, regio-, and stereoselective hydroformylation, *Synthesis* (2001) 1–36.

2. Frohning, C. D. and Kohlpaintner, C. W., In: *Applied homogeneous catalysts with organometallic compounds*, Eds. B. Cornils and W. A. Herrmann, Vol. 1, VCH, Weinheim 1996, Ch. 2.1.

3. Van Leeuwen, P. W. N. M. and Clawer, C., Eds., *Rhodium catalyzed hydroformylation,* In *Catalysis by metal complexes*, Vol. 22, Kluwer, Dordrecht 2000, 284 p.

4. Beller, M., Cornils, B., Frohning, C. D. and Kohlpaintner, C. W., Progress in hydroformylation and carbonylation, Review, *J. Mol. Catal. A* **104** (1995) 17–85.

5. Reinius, H., *Activity and selectivity in hydroformylation: role of ligand, substrate and process conditions*, Doctoral thesis, Industrial Chemistry Publication Series, No. 9, Espoo 2001, 52 p.

6. Tudor, R. and Ashley, M., Enhancement of industrial hydroformylation processes by the adoption of rhodium-based catalyst: Part II Key improvements to rhodium process, and use in non-propylene applications, *Platinum Metals Rev.* **51** (2007) 164–171.

7. Likholobov, V. A. and Moroz, B. L., In *Handbook of heterogeneous catalysis*, Eds. G. Ertl, H. Knözinger and J. Weitkamp, Vol. 5, VCH, Weinheim 1997, Ch. 4.5.

8. Zhao, J., Zhang, Y., Han, J. and Jiao, Y., Preparation and performance of anchored heterogenised rhodium complex catalyst for hydroformylation, J. Mol. Catal. A: Chem. 241 (2005) 238–243.

9. Mukhopadhyay, K., Mandale, A. B. and Chaudhari, R. V., Encapsulated $HRh(CO)(PPh_3)_3$ in microporous and mesoporous supports: novel heterogeneous catalysts for hydroformylation, *Chem. Mater.* **15** (2003) 1766–1777.

10. Feldman, J. and Orchin, M., Membrane-supported rhodium hydroformylation catalysts, *J. Mol. Catal.* **63** (1990) 213–221.

11. Ro, K. S. and Woo, S. I., Hydroformylation of propylene catalyzed over polymer-immobilized $RhCl(CO)(PPh_3)_2$: Effect of crosslink ratio and FTIR study, *J. Mol. Catal.* **61** (1990) 27–39.

12. Arai, H., Hydroformylation, hydrogenation and isomerization of olefins over polymer-immobilized rhodium complexes, *J. Catal.* **51** (1978) 135–142.

13. Terekhova, G. V., Kolesnichenko, N. V., Alieva, E. D., Truhmanova, N. I., Teleshev, A. T., Markova, N. A., Alekseeva, E. I., Slivinsky, E. V., Loktev, S. M. and Pesin, O. Y., Rhodium carbonyl catalysts, immobilized on polymeric supports in the hydroformylation of olefins, In *Preparation of catalysts VII*, *Stud. Surf. Sci. Catal.* **118** (1998) 255–263.

14. Pittman, C. U., Jr., and Wilemon, G. M., 1-pentene hydroformylation catalyzed by polymer-bound ruthenium complexes, *J. Org. Chem.* **46** (1981) 1901–1905.

15. Terreros, P., Pastor, E. and Fierro J. L. G., Hept-1-ene hydroformylation on phosphinated polystyrene-anchored rhodium complexes, *J. Mol. Catal.* **53** (1989) 359–369.

16. Junfan, W., Juntan, S., Hong, L. and Binglin, H., The stability of a polymer-supported rhodium complex in the batch hydroformylation of 1-hexene, *Reactive Polymers* **12** (1990) 177–186.

17. Pittman, C. U., Jr., and Honnick, W. D., Rhodium-catalyzed hydroformylation of allyl alcohol. A potential route to 1,4-butanediol, *J. Org. Chem.* **45** (1980) 2132–2139.

18. Jongsma, T., Kimkes, P., Challa, G. and van Leeuwen, P. W. N. M., A new type of highly active polymer-bound rhodium hydroformylation catalyst, *Polymer* **33** (1992) 161–165.

19. Bonaplata, E., Ding, H., Hanson, B. E. and McGrath, J. E., Hydroformylation of 1-octene with a poly(arylene ether triaryl phosphine) rhodium complex, *Polymer* **36** (1995) 3035–3039.

20. Hartley, F. R., Murray, S. G. and Nicholson, P. N., γ-radiation-produced supported metal complex catalysts. IV. Rhodium(I) hydroformylation catalysts supported on phosphinated polypropylene, *J. Mol. Catal.* **16** (1982) 363–383.

21. Evans, G. O., Pittman, C. U., Jr., McMillan, R., Beach, R. T. and Jones, R., Synthetic and catalytic studies of polymer-bound metal carbonyls, *J. Organom. Chem.* **67** (1974) 295–314.

22. Lenarda, M., Storaro, L. and Ganzerla, R., Hydroformylation of simple olefins catalyzed by metals and clusters supported on unfunctionalized inorganic carriers, Review, *J. Mol. Catal. A: Chem.* **111** (1996) 203–237.

23. Reinikainen, M., *Cobalt and ruthenium-cobalt catalysts in CO hydrogenation and hydroformylation*, Doctoral thesis, Technical Research Centre of Finland (VTT), Espoo 1998, 64 p.

24. Ungváry, F., Review, Application of transition metals in hydroformylation annual survey covering the year 2004, *Coord. Chem. Reviews* **249** (2005) 2946–2961.

25. Li, B., Li, X., Asami, K. and Fujimoto, K., Hydroformylation of 1-hexene over rhodium supported on active carbon catalyst, *Chem. Lett.* **32** (2003) 378–379.

26. Yan, L., Ding, Y. J., Zhu, H. J., Xiong, J. M., Wang, T., Pan, Z. D. and Lin, L. W., Ligand modified real heterogeneous catalysts for fixed-bed hydroformylation of propylene, *J. Mol. Catal. A: Chem*. **234** (2005) 1–7.

27. Zhu, H., Ding, Y., Yan, L., Lu, Y., Li, C., Bao, X. and Lin, L., Recyclable heterogeneous Rh/SiO_2 catalyst enhanced by organic PPh_3 ligand, *Chem. Lett.* **33** (2004) 630–631.

28. Zhang, Y., Zhang, H. -B., Lin, G. -D., Chen, P., Yuan, Y. -Z. and Tsai, K. R., Preparation, characterization and catalytic hydroformylation properties of carbon

nanotubes-supported Rh-phosphine catalyst, *Appl. Catal. A: Gen.* **187** (1999) 213–224.

29. Andersson, C., Nikitidis, A., Hjortkjær, J. and Heinrich, B., Continuous liquid-phase hydroformylation of 1-hexene with a poly-TRIM bound rhodium-phosphine complex, *Appl. Catal. A: Gen*. **96** (1993) 345–354.

30. Davis, M. E., Butler, P. M., Rossin, J. A. and Hanson, B. E., Hydroformylation of 1-hexene by soluble and zeolite-supported rhodium species, *J. Mol. Catal*. **31** (1985) 385–395.

31. Falbe, J., Ed., *New syntheses with carbon monoxide*, Springer-Verlag, Heidelberg 1980, 465 p.

32. Henrici-Olivé, G. and Olivé, S., *The chemistry of the catalysed hydrogenation of carbon monoxide*, Springer-Verlag, Berlin 1984, 231 p.

33. Balakos, M. W. and Chuang, S. S. C., Transient response of propionaldehyde formation during $CO/H_2/C_2H_4$ reaction on Rh/SiO_2, *J. Catal.* **151** (1995) 253–265.

34. Huang, L., Xu, Y., Guo, W., Liu, A., Li, D. and Guo, X., Study on catalysis by carbonyl cluster-derived SiO_2-supported rhodium for ethylene hydroformylation, *Catal. Lett.* **32** (1995) 61–81.

35. Chuang, S. S. C. and Pien, S. I., Infrared study of the CO insertion reaction on reduced, oxidised, and sulfided Rh/SiO_2 catalysts, *J. Catal.* **135** (1992) 618–634.

36. Sachtler, W. M. H. and Ichikawa, M., Catalytic sites requirements for elementary steps in syngas conversion to oxygenates over promoted Rh, *J. Phys. Chem.* **90** (1986) 4752–4758.

37. Hedrick, S. A., Chuang, S. S. C. and Brundage, M. A., Deuterium pulse transient analysis for determination of heterogeneous ethylene hyroformylation mechanistic parameters, *J. Catal.* **185** (1999) 73–90.

38. Chuang, S. S. C., Stevens, R. W., Jr. and Khatri, R., Mechanism of C_{2+} oxygenate synthesis on Rh catalysts, *Topics in Catal*. **32** (2005) 225–232.

39. Hakuli, A., *Preparation and characterization of supported CrO_x catalysts for butane dehydrogenation*, Doctoral thesis, Helsinki University of Technology, Espoo 1999, 48 p.

40. Puurunen, R., *Preparation by atomic layer deposition and characterisation of catalyst supports surfaced with aluminium nitride*, Doctoral thesis, Industrial Chemistry Publication Series, No. 13, Espoo 2002, 78 p.

41. Backman, L. B., Rautiainen, A., Krause, A. O. I. and Lindblad, M., A novel Co/SiO_2 catalyst for hydrogenation, *Catal. Today* **43** (1998) 11–19.

42. Halttunen, M. E., Niemelä, M. K., Krause, A. O. I., Vaara, T. and Vuori, A. I., Rh/C catalysts for methanol carbonylation I. Catalyst characterisation, *Appl. Catal. A: Gen.* **205** (2001) 37–49.

43. Näsman, J. H., Sundell, M. J. and Ekman, K. B., *Process for the preparation of a graft copolymer bound catalyst*, US Patent 5326825, Jul. 5, 1994.

44. Dietz, W. A., Response factors for gas chromatographic analyses, *J. Gas. Chromatogr.* **5** (1967) 68–71.

45. Takeuchi, K, Hanaoka, T. Matsuzaki, T., Reinikainen, M. and Sugi, Y., Selective vapor phase hydroformylation of ethylene over cluster-derived cobalt catalysts, *Catal. Lett.* **8** (1991) 253–261.

46 . Matsuzaki, T., Hanaoka, T. Takeuchi, K., Arakawa, H., Sugi, Y., Wei, K., Dong, T. and Reinikainen, M., Oxygenates from syngas over highly dispersed cobalt catalysts, *Catal. Today* **36** (1997) 311–324.

47. Reuel, R. and Bartholomew, C., The stoichiometries of H_2 and CO adsorptions on cobalt: effects of support and preparation, *J. Catal.* **85** (1984) 63–77.

48. Reuel, R. and Bartholomew, C., Effects of support and dispersion on the CO hydrogenation activity/selectivity properties of cobalt, *J. Catal.* **85** (1984) 78–88.

49. Niemelä, M. K., Backman, L., Krause, A. O. I. and Vaara, T., The activity of the Co/SiO_2 catalyst in relation to pretreatment, *Appl. Catal. A: Gen.* **156** (1997) 319–334.

50. Alvila, L., Pakkanen, T. A., Pakkanen, T. T. and Krause, O., Hydroformylation of olefins catalysed by rhodium and cobalt clusters supported on organic (Dowex) resins, *J. Mol. Catal.* **71** (1992) 281–290.

51. Cao, S.-K., Huang, M.-Y. and Jiang, Y.-Y., Hydroformylation of heptene-1 catalyzed by some inorganic polymer-metal complexes, *J. Macromol. Sci., Chem. A* **26** (1989) 381–389.

52. Omata, K., Fujimoto, K., Shikada, T. and Tominaga, H., Vapor-phase carbonylation of organic compounds over supported transition-metal catalyst. 6. On the character of nickel/active carbon as methanol carbonylation catalyst, *Ind. Eng. Chem. Res.* **27** (1988) 2211–2213.

53. Halttunen, M. E., Niemelä, M. K., Krause, A. O. I. and Vuori, A. I., Rh/C catalysts for methanol hydrocarbonylation II. Activity in the presence of MeI, *Appl. Catal. A: Gen.* **182** (1999) 115–123.

54. Tomita, A. and Tamai, Y., Hydrogenation of carbons catalysed by transition metals, *J. Catal.* **27** (1972) 293–300.

55. Matsuzaki, T., Hanaoka, T., Takeuchi, K. Sugi, Y. and Reinikainen, M., Effects of modification of highly dispersed cobalt catalysts with alkali cations on the hydrogenation of carbon monoxide, *Catal. Lett.* **10** (1991) 193–199.

56. Halttunen, M. E., Niemelä, M. K., Krause, A. O. I. and Vuori, A. I., Some aspects on the losses of metal from the support in the hydrocarbonylation of methanol, *J. Mol. Catal. A:Chem.* **144** (1999) 307–314.

57. Kiviaho, J., Niemelä, M. K., Reinikainen, M., Vaara, T. and Pakkanen, T. A., The effect of decomposition atmosphere on the activity and selectivity of the carbonyl cluster derived Co/SiO_2 and Rh/SiO_2 catalysts, *J. Mol. Catal. A: Chem.* **121** (1997) 1–8.

58. Takahashi, N., Takeyama, T., Fujimoto, T., Fukuoka, A. and Ichikawa, J., Formation of Rh carbonyl cluster species and its conversion into metal particles during exposure of Rh/active carbon to carbon monoxide revealed by EXAFS and TPD techniques, *Chem. Lett.* (1992) 1441–1444.

59. Guyot, A., Hodge, P., Sherrington, D. C., and Widdecke, H., Recent studies aimed at the development of polymer-supported reactants with improved accessibility and capacity, *React. Polym.* **16** (1991/1992) 233–259.

60. Karinen, R. S., Krause, A. O. I., Ekman, K., Sundell, M. and Peltonen, R., Etherification over a novel acid catalyst, *Stud. Surf. Sci. Catal.* **130** (2000) 3411–3416.

61. Babich, I. V., Plyuto, Y. V., Van der Voort, P. and Vansant, E. F., Thermal transformations of chromium acetylacetonate on silica surface, *J. Colloid and Interf. Sci.* **189** (1997) 144–150.

62. Mikami, M., Nakagawa, I. and Shimanouchi, T., Far infra-red spectra and metal-ligand force constants of acetylacetonates of transition metals, *Spectrochim. Acta* **23A** (1967) 1037–1053.

63. Van Leeuwen, P. W. N. M., Decomposition pathways of homogeneous catalysts, *Appl. Catal. A: Gen*. **212** (2001) 61–81.

64. Hakuli, A. and Kytökivi, A., Binding of chromium acetylacetonate on a silica support, *Phys. Chem. Chem. Phys.* **1** (1999) 1607–1613.

65. Cowie, J. M. G., *Polymers: chemistry and physics of modern materials*, 2nd Ed.,. Blackie Academic & Professional, London, 1991, 436 p.

66. Fessenden, R. J. and Fessenden, J. S., *Organic chemistry*, 4th Ed., Brooks/Cole, Pacific Grove 1990, pp. 542–543.

67. Zhang, Y., Nagasaka, K., Qiu, X. and Tsubaki, N., Hydroformylation of 1-hexene for oxygenate fuels on supported cobalt catalysts, *Catal. Today* **104** (2005) 48–54.

68. Niemelä, M., Krause, O., Vaara, T., Kiviaho, J. and Reinikainen, M., The effect of precursor on the characteristics of Co/SiO_2 catalysts, *Appl. Catal. A: Gen.* **147** (1996) 325–345.

69. Etspüler, A. and Suhr, H., Deposition of thin rhodium films by plasma-enhanced chemical vapour deposition, *Appl. Phys. A* **48** (1989) 373–375.

70. Flint, E. B., Messelhäuser, J. and Suhr, H., Laser-induced CVD or rhodium, *Appl. Phys. A* **53** (1991) 430–436.

71. Jesse, A. C., Ernsting, J. M., Stufkens, D. J. and Vrieze, K., Vapour pressure measurements on (acac)M(substituted olefin)$_2$ and (acac)M(CO)$_2$ (M=Rh(I), Ir(I)), *Thermochim. Acta* **25** (1978) 69–75.

INDUSTRIAL CHEMISTRY PUBLICATION SERIES

No. 1 Niemelä, M.,
Catalytic reactions of synthesis gas. Part I: Methanation and CO Hydrogenation. 1992.

No. 2 Niemelä, M.,
Catalytic reactions of synthesis gas. Part II: Methanol carbonylation and homologation. 1993.

No. 3 Saari, E.,
Substituoitujen bentseenien hapen-, rikin- ja typenpoisto vedyllä. 1994.

No. 4 Niemelä, M.,
Catalytic reactions of synthesis gas. Part III: Determination of reaction kinetics. 1993.

No. 5 Niemelä, M.,
Catalytic reactions of synthesis gas. Part IV: Heterogeneous hydroformylation. 1994.

No. 6 Perä, M.,
Activated carbon as a catalyst support. 1995.

No. 7 Halttunen, M.,
Hydrocarbonylation of alcohols, carboxylic acids and esters. 1996.

No. 8 Puurunen, R.,
Trimetyylialumiinin ja ammoniakin reaktiot alumiininitridin valmistuksessa: kirjallisuuskatsaus. 2000.

No. 9 Reinius, H.,
Activity and selectivity in hydroformylation: Role of ligand, substrate and process conditions. 2001.

No. 10 Harlin, E.,
Molybdenum and vanadium oxide catalysts in the dehydrogenation of butanes. 2001.

No. 11 Viljava, T.-R.,
From biomass to fuels: Hydrotreating of oxygen-containing feeds on a $CoMo/Al_2O_3$ hydrodesulfurization catalyst. 2001.

No. 12 Karinen, R.,
Etherification of some C_8-alkenes to fuel ethers. 2002.

No. 13 Puurunen, R.,
Preparation by atomic layer deposition and characterisation of catalyst supports surfaced with aluminium nitride. 2002.

No. 14 Rautanen, P.,
Liquid phase hydrogenation of aromatic compounds on nickel catalyst. 2002.

No. 15 Pääkkönen, P.,
Kinetic studies on the etherification of C_5-alkenes to fuel ether TAME. 2003.

No. 16 Kanervo, J.,
Kinetic analysis of temperature-programmed reactions. 2003.

No. 17 Lylykangas, M.,
Kinetic modeling of liquid phase hydrogenation reactions. 2004.

No. 18 Lashdaf, M.,
Preparation and characterisation of supported palladium, platinum and ruthenium catalysts for cinnamaldehyde hydrogenation. 2004.

No. 19 Airaksinen, S.,
Chromium oxide catalysts in the dehydrogenation of alkanes. 2005.

No. 20 Honkela, M.,
Dimerisation of isobutene on acidic ion-exchange resins. 2005.

No. 21 Sippola, V.,
Transition metal-catalysed oxidation of lignin model compounds for oxygen delignification of pulp. 2006.

No. 22 Maunula, T.,
NO_x reduction by hydrocarbons and hydrogen on metal oxide and zeolite based catalysts in lean conditions. 2007.

No. 23 Keskitalo, T.,
Modelling of chemical reaction kinetics with data from temperature-programmed experiments. 2007.

No. 24 Zeelie, T.,
Rhodium and cobalt catalysts in the heterogeneous hydroformylation of ethene, propene and 1-hexene. 2007.

ISBN 978-951-22-9024-6
ISSN 1235-6840